

**Synthesis and Characterization of Novel Glyceline-based
Low Transition Temperature Mixtures (LTTM) with L-Arginine**

by

Hor Jun You

14871

Dissertation submitted in partial fulfilment of

the requirements for the

BACHELOR OF ENGINEERING (HONS)

CHEMICAL ENGINEERING

JANUARY 2015

Universiti Teknologi PETRONAS

32610, Bandar Seri Iskandar

Perak Darul Ridzuan

CERTIFICATION OF APPROVAL

Synthesis and Characterization of Novel Glyceline-based Low Transition Temperature Mixtures (LTTM) with L-Arginine

by

Hor Jun You

14871

A project dissertation submitted to the
Chemical Engineering Programme
Universiti Teknologi PETRONAS
in partial fulfilment of the requirement for the
BACHELOR OF ENGINEERING (HONS)
(CHEMICAL ENGINEERING)

Approved by,

Prof. Dr. Thanabalan Murugesan

UNIVERSITI TEKNOLOGI PETRONAS
BANDAR SERI ISKANDAR, PERAK
JANUARY 2015

CERTIFICATION OF ORIGINALITY

This is to certify that I am responsible for the work submitted in this project, that the original work is my own except as specified in the references and acknowledgements, and that the original work contained herein have not been undertaken or done by unspecified sources or persons.

HOR JUN YOU

ACKNOWLEDGEMENT

I would like to express my heartfelt gratitude to my supervisor, Prof. Dr. Thanabalan Murugesan for giving me the opportunity to do this project on the topic of Synthesis and Characterization of Novel Glycine-based Low Transition Temperature Mixtures (LTTM) with L-Arginine. Through his guidance and encouragement, the project has been successfully accomplished.

Furthermore, I am sincerely grateful to those who have helped me in giving constructive criticism and friendly advice during the project work, especially Ms. Fareeda Chemat. Nevertheless, I express my warm thanks to all the examiners and judges of Poster Presentation for sharing their illuminating views on a number of issues related to the project.

Lastly, I would also like to thank my parents and friends who have encouraged and supported me throughout the process.

ABSTRACT

Novel low transition temperature mixtures (LTTM) based on three different mole ratio of hydrogen bond donor (HBD) in glyceline of (choline chloride: glycerol) 1:2, 1:3, and 1:4 with L-arginine (L-Arg) are successfully synthesized with different mole ratios between glyceline to L-Arg. The melting point of LTTM are not detected, however glass transition temperature are observed. The physical properties, such as density, viscosity, and refractive index of LTTM are measured at atmospheric pressure and temperature from (298.15 up to 343.15) K at an interval of 5K. The results showed that different mole ratio of HBD in glyceline, the mole ratio of glyceline to L-Arg, and temperature have great influences on both the physical and thermal properties of LTTM. Densities and viscosities of LTTM formed by glyceline and L-Arg decrease with increase temperature, but increase with increase of HBD and L-Arg mole ratio. The refractive indexes of LTTM decrease with increase temperature and HBD mole ratio but increase with decrease L-Arg mole ratio. The temperature dependence of densities and refractive indexes for LTTM are correlated by an empirical linear functions, and the viscosities are fitted using Vogel-Tamman-Flucher (VTF) equation and are found that R^2 of all regression equations are 0.9999 and above.

TABLE OF CONTENTS

CERTIFICATION OF APPROVAL	i
CERTIFICATION OF ORIGINALITY	ii
ACKNOLEDGEMENT	iii
ABSTRACT	iv
LIST OF FIGURES	vii
LIST OF TABLES	ix

CHAPTER 1

INTRODUCTION	1
1.1 Background	1
1.2 Problem Statement.....	3
1.3 Objectives.....	4
1.4 Scope of Study.....	4

CHAPTER 2

LITERATURE REVIEW AND THEORY	6
2.1 Room-Temperature Ionic Liquids (RTIL), Deep Eutectic Solvents (DES) and Low Transition Temperature Mixtures (LTTM).....	6
2.2 Physical Properties Characterization	9
2.2.1 Melting Point (MP)	9
2.2.2 Glass Transition Temperature (T_g).....	12
2.2.3 Density, Viscosity and Refractive Index	15
2.3 Material Selection	20
2.3.1 Choline Chloride (ChCl)	20
2.3.2 Glycerol (Gly).....	21
2.3.3 L-Arginine (L-Arg)	22

CHAPTER 3

METHODOLOGY/PROJECT WORK.....	25
--------------------------------------	-----------

3.1	Materials and Apparatus	25
3.2	Methodology	26
3.2.1	Synthesis of LTTM System	26
3.2.2	Characterization of LTTM.....	26
3.3	Project Feasibility	27
3.4	Gantt Chart and Key Milestones.....	28
 CHAPTER 4		
RESULT AND DISCUSSION		30
4.1	Formation of Solvents	30
4.2	Water Content.....	33
4.3	Thermal Properties.....	34
4.3.1	Decomposition Temperature	34
4.3.2	Melting Point / Glass Transition Temperature (MP / T _g)	37
4.4	Physical Properties.....	39
4.4.1	Density	39
4.4.2	Viscosity	42
4.4.3	Refractive Index.....	46
 CHAPTER 5		
CONCLUSION		50
 REFERENCES		
APPENDICES		

LIST OF FIGURES

Figure 1. World CO ₂ emissions from 1971 to 2012 by fuel (MT of CO ₂) [4]	1
Figure 2. Amines forming stable carbamates or bicarbonates with CO ₂ [9].....	2
Figure 3. Structures of some halide salts and hydrogen bond donors used in the formation of deep eutectic solvents [31]	8
Figure 4. Schematic representation of a eutectic point on a two component phase diagram [31]	9
Figure 5. Correlation between the freezing temperature and the depression of freezing point for metal salts and amides when mixed with choline chloride in 2:1 ratio, where the individual points represent different mixture [31]	10
Figure 6. Schematic representation of exceptional cases of two eutectic points on a two component phase diagram [35]	12
Figure 7. Measurement / Prediction of T _g by DSC.....	13
Figure 8. T _g against different molar ratio of Gly observed for the DES between K ₂ CO ₃ and Gly ratios studied in [30]	14
Figure 9. DSC curves showing the trend of T _g for different lactic acid: choline chloride ratios [29]	15
Figure 10. Density of ChCl: Gly (1:2) as a function of pressure at different temperatures: ●, 298.15 K; ■, 303.15 K; ▲, 308.15 K; ▼, 313.15 K; ◀, 318.15 K; ▶, 323.15 K [40].....	17
Figure 11. Shear rate–dependent viscosity of 1:2:6 ChCl: Gly: 1,5-Diazabicyclo[4.3.0]non-5-ene (DBN) measured at 298.15K [42]	18
Figure 12. Viscosity change with temperature for lactic acid: choline chloride LTTM at different molar ratios: ●, 1.3:1; ○, 1.5:1; ▼, 2:1; △, 3:1; ■, 5:1; □, 10:1 [29] ..	18

Figure 13. Dynamic viscosity of selected DES containing K_2CO_3 and Gly (1:4, 1:5, 1:6) as function of temperature [30]	19
Figure 14. Plot of temperature versus surface tension for different concentration of glycerol in DES [43]	20
Figure 15. IUPAC structure of ChCl [44]	20
Figure 16. IUPAC structure of Gly [44]	21
Figure 17. IUPAC structure of L-Arg in its un-ionized form.....	22
Figure 18. Delocalization of charge in guanidinium group of L-Arg [48]	23
Figure 19. Grouped table of 21 amino acids' structures, nomenclature, and their side groups' pKa values [48].....	24
Figure 20. Graph of molar ratio of arginine against molar ratio of glycerol	32
Figure 21. TGA curves of DES / LTTM.....	36
Figure 22. DES scanning program for all DES / LTTM.....	38
Figure 23. DSC curves of DES / LTTM	38
Figure 24. Density of DES against temperature range (298.15-343.15) K.....	42
Figure 25. Viscosity of DES against temperature range (298.15-343.15) K	43
Figure 26. $\ln \eta$ against $1/T$ plot for all DES.....	46
Figure 27. Refractive index of DES against temperature range (298.15-333.15) K .	49

LIST OF TABLES

Table 1. General Formula for the Classification of DES [31].....	7
Table 2. MP of a selection of DES [26, 31, 34]	11
Table 3. Physical properties of DES at 298K [26, 31].....	16
Table 4. RI of ChCl: ethylene glycol (Eth) and ChCl: Gly DES [41]	19
Table 5. Properties of ChCl [44]	21
Table 6. Properties of Glycerol [44]	22
Table 7. Properties of common amino acids with polar side chain [48].....	23
Table 8. Equipment list for the project	25
Table 9. Gantt chart with key milestones.....	28
Table 10. Eutectic solvents formed with arginine and glyceline of different ratio ...	30
Table 11. Mass of individual component of glyceline for mixing	33
Table 12. Mass of individual component of LTTM for mixing	33
Table 13. Water content of DES.....	34
Table 14. Decomposition temperature data of DES	36
Table 15. Density versus temperature data for DES (1:2, 1:2 (lit.), 1:2:0.1 and 1:2:0.2) over the temperature range (298.15-343.15) K	39
Table 16. Density versus temperature data for DES (1:3, 1:3:0.1 and 1:3:0.2) over the temperature range (298.15-343.15) K.....	40
Table 17. Density versus temperature data for DES (1:4, 1:4:0.1 and 1:4:0.2) over the temperature range (298.15-343.15) K.....	41

Table 18. Result of regression analysis of density versus temperature data according to equation for DES over the temperature range (298.15-343.15) K	41
Table 19. Viscosity versus temperature data for DES (1:2, 1:2 (lit.), 1:2:0.1 and 1:2:0.2) over the temperature range (298.15-343.15) K	43
Table 20. Viscosity versus temperature data for DES (1:3, 1:3:0.1 and 1:3:0.2) over the temperature range (298.15-343.15) K	44
Table 21. Viscosity versus temperature data for DES (1:4, 1:4:0.1 and 1:4:0.2) over the temperature range (298.15-343.15) K	44
Table 22. Result of regression analysis of $\ln \eta$ versus $1/T$ according to equation for DES over the temperature range (298.15-343.15) K	45
Table 23. Refractive index versus temperature data for DES (1:2, 1:2 (lit.), 1:2:0.1 and 1:2:0.2) over the temperature range (298.15-333.15) K	47
Table 24. Refractive index versus temperature data for DES (1:3, 1:3:0.1 and 1:3:0.2) over the temperature range (298.15-333.15) K	47
Table 25. Refractive index versus temperature data for DES (1:4, 1:4:0.1 and 1:4:0.2) over the temperature range (298.15-333.15) K	48
Table 26. Result of regression analysis of refractive index versus temperature data according to equation for DES over the temperature range (298.15-333.15) K	48

CHAPTER 1

INTRODUCTION

1.1 Background

It is undeniable that global warming is occurring. Recent bloom in energy production and consumption has led to major climate change [1, 2]. The reason, as many scientist and researchers believe, is the emission of greenhouse gases (GHGs), such as carbon dioxide (CO_2), nitrous oxide (N_2O) and methane (CH_4), into the atmosphere. Among these GHGs, CO_2 is the largest contributor in regards to its amount present in the atmosphere contributing to about 60% of the global warming effects [3]. Comparing to year 1971, the annual release of CO_2 has been doubled from 15,633 metric tonne (MT) to 31,734 MT within 40 years of time [4]. As of October 2014, the atmospheric CO_2 has reached concentration of 395.93 parts per million (ppm) [5], the highest since 800,000 years ago and likely the highest in the past 20 million years [6].

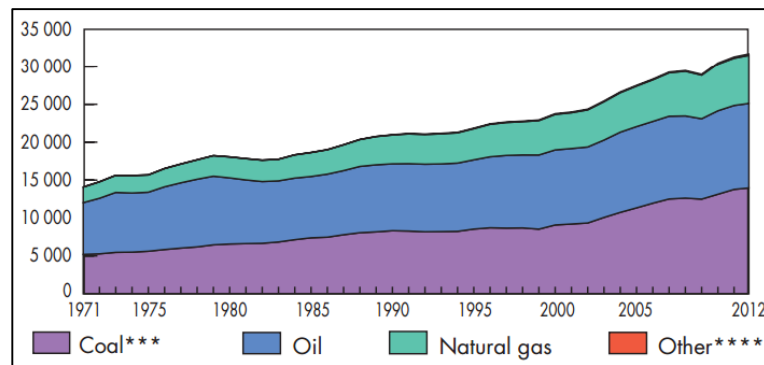


Figure 1. World CO₂ emissions from 1971 to 2012 by fuel (MT of CO₂) [4]

Despite the growth in renewable energy, fossil fuels will continue to be the dominant source of energy through to 2050, especially in countries like China and India [7]. With the current domination of low carbon fossil fuel (i.e. natural gas), renewable energies are not expected to replace fossil fuels as early as 2075 [7]. Therefore, CO₂ capture and sequestration from industrial flue are drawing increasing attention as a potential method for controlling greenhouse gas emissions.

Among different developed methods, the post-combustion capture has the advantage that it can be applied to retrofit the existing plants. Physical absorption such as Selexol, Rectisol, Fluor; chemical absorption such as potassium carbonate; membrane separation; adsorption through zeolite; and cryogenic distillation are among the current developed technology for CO₂ capture and sequestration [8]. Currently, the cheapest and most mature technology for the CO₂ post-combustion capture is the amine-based absorption (i.e. Alkanolamines) [9, 10]. Due to its high affinity to CO₂, regeneration of solvent will demand an intensive energy use to break the chemical bonds between the absorbents and the absorbed CO₂ [11, 12]. Besides, the utilization of amine based solvent has several serious drawbacks including high equipment corrosion, and high cost in the operations [13, 14]. Therefore, it is of benefit to find alternative solvents that compromise the high affinity for CO₂ with the ease of solvent regeneration and reuse.

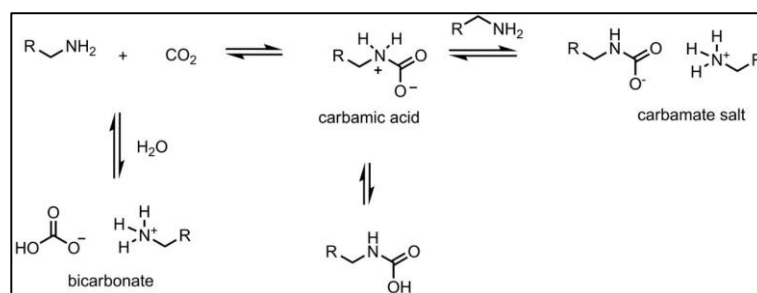


Figure 2. Amines forming stable carbamates or bicarbonates with CO₂ [9]

In recent study, the ability of room-temperature ionic liquids (RTIL) to absorb CO₂ is found superior compared to other organic solvents proposed [15]. RTIL composed of large, delocalized cations and anions which has low vapour

pressure, high thermal and chemical stability, non-flammability, and high solvation capacity [16-19]. Their unique properties characterized by modifying cations and anions, make them an ideal class of separation media [20-23]. However, they have not been widely used because of difficulty in synthesis, high cost in bulk application and low tolerance to moisture. In addition to that, some studies proven that RTIL is not inherently green due to their toxic nature [24, 25].

To overcome the limitations and challenges of RTIL, both deep eutectic solvents (DES) and low transition temperature mixtures are put forward as versatile alternatives [26]. Being the next generation of ionic liquids, they are prepared by mixing substituted quaternary halide salt or metal salt with hydrogen bond donors (HBD) in which at the eutectic point, maximum depression of melting point will significantly alter the physical appearance of compound at room temperature [27]. DES consist of at least one HBD and one hydrogen bond acceptor (HBA) counterpart. Their properties can be adjusted by selecting the nature and ratio of the hydrogen bond counterparts. They often share many interesting characteristics with green solvents RTIL with the outstanding features of low price and biodegradability [28]. Unlike DES, LTTM is unlikely to show its glass transition temperature before melting point. It is a recent discovery through the mixture of lactic acid (LA) and choline chloride [29] as well as potassium carbonate (K_2CO_3) and glycerol (Gly) [30].

1.2 Problem Statement

The current DES and LTTM is dominant by the binary mixtures between halide salts and HBD (i.e. choline chloride (ChCl) and urea) [28, 31]. DES and LTTM have been recognized as a cost effective alternative to RTIL as it possess several advantages over traditional RTIL and can be prepared easily in high purity at low cost. In addition, they are non-toxic, have no reactivity with water and being biodegradable. However, the carbon dioxide (CO_2) absorption rate of DES and LTTM is very low compare to task specified RTIL [15]. It is important to find a feasible alternatives to the expensive RTIL, while shorten the performance gap between DES and LTTM with the current amine adsorption technology.

Recently, there are research papers published discussing the potential of the third compounds to be mixed into DES to form a new DES or LTTM. Acids, alkalis, sugar, amine, salts are among the suggested third component [32]. New DES and LTTM are synthesized every day but most of them are not well characterized due to over focus on CO₂ adsorption rate. Density, refractive index and viscosities are among the important characterization that requires more attention [33] since these data are essential in equipment design, operation parameter settings and quality assurances for mass production.

1.3 Objectives

The objective of the project includes, but not limited to:

- To identify suitable components for the DES and LTTM
- To identify molar ratio between components that will form new DES or LTTM
- To characterize the produced DES or LTTM using various analytical tools

1.4 Scope of Study

The variation of ternary compounds of DES and LTTM will result in different eutectic mixing molar ratio, different physical properties and different level of performance of CO₂ absorption. The characteristics of a decent LTTM that will be observed are low melting point, low viscosity and high selectivity towards CO₂. First, the suitable ternary component is determined based on literature study and preliminary mixing. Then, the eutectic mixing molar ratio between ChCl, Gly and ternary component can be determined by trial and error method. Next, the effects of ternary components in DES and LTTM will be studied such as CO₂ absorption and physical properties. Test will be performed on the resulted DES and LTTM, with different molar percentage of ternary components in order to determine the eutectic mixing ratio and their qualities. Resulted DES and LTTM is considered success as long as colourless clear solution formed within acceptable time frame.

Characterization of physical properties include, but not limited to thermal gravimetric analysis (TGA) test, and differential scanning calorimetry (DSC) test for thermal stability and determination of melting point or glass transition temperature; density, viscosity, and refractive index.

CHAPTER 2

LITERATURE REVIEW AND THEORY

2.1 Room-Temperature Ionic Liquids (RTIL), Deep Eutectic Solvents (DES) and Low Transition Temperature Mixtures (LTTM)

RTIL is a class of fluid which solely consists of ions and are liquid at room temperatures. RTIL is split into two distinct categories, which are those formed from eutectic mixtures of metal halides (i.e. AlCl_3 and ZnCl_2) [22] and organic salts (generally nitrogen based and predominantly with halide anions), as well as those containing discrete anions such as PF_6 or bis-(trifluoromethanesulphonyl) imide. The first generation of RTIL is fluid at low temperatures due to the formation of bulky chloroaluminate or chlorozincate ions while the second generation of RTIL is those that are entirely composed of discrete ions. A series of Alkylimidazolium RTIL is discovered to be more stable with the presents of air and moisture when AlCl_3 is replaced with discrete anions such as the tetrafluoroborate and acetate moieties. [27] However, moisture in the air can easily upset the chemical and physical properties of RTIL, with the development of HF as water content increases [28]. The system can be further improved by using more hydrophobic anions such as trifluoromethanesulfonate (CF_3SO_3^-), bis-(trifluoromethanesulphonyl)imide [$(\text{CF}_3\text{SO}_2)_2\text{N}^-$], and tris-(trifluoromethanesulphonyl)methide [$(\text{CF}_3\text{SO}_2)\text{C}^-$] [28–30]. It is estimated that the total number of possible RTIL could be in the range of 10^6 distinct systems. RTIL has the potential to be highly versatile solvents, with properties which can be easily tuned for specific uses. However, RTIL is not successful alternatives to current aqueous sorbent as they are neither simple nor economic to synthesize. [31]

DES and LTTM are emerging as a new class of green solvent related to RTIL, sharing many of their favourable characteristics, such as low cost, minimum volatility, biodegradability, non-flammable, and high thermal stability [23–31]. DES is typically formed from two or more compounds capable of intermolecular interactions, particularly through hydrogen bonding. Generally, DES can be described using the general formula, $\text{Cat}^+\text{X}^-\text{zY}$ where Cat^+ is in principle any ammonium, phosphonium, or sulfonium cation, and X is a Lewis base, generally a halide anion. The complex anionic species are formed between X^- and either a Lewis or Brønsted acid Y (z refers to the number of Y molecules that interact with the anion). The majority of studies have focused on quaternary ammonium and imidazolium cations with particular emphasis being placed on more practical systems using choline chloride, $[\text{ChCl}, \text{HOC}_2\text{H}_4\text{N}^+(\text{CH}_3)_3\text{Cl}^-]$. DES is largely classified depending on the nature of the compound used (Table 1).

Table 1. General Formula for the Classification of DES [31]

Type	General Formula	Terms
I	$\text{Cat}^+\text{X}^-\text{zMCl}_x$	$\text{M} = \text{Zn, Sn, Fe, Al, Ga, In}$
II	$\text{Cat}^+\text{X}^-\text{zMCl}_x \cdot y\text{H}_2\text{O}$	$\text{M} = \text{Cr, Co, Cu, Ni, Fe}$
III	$\text{Cat}^+\text{X}^-\text{zRZ}$	$\text{Z} = \text{CONH}_2, \text{COOH, OH}$
IV	$\text{MCl}_x + \text{RZ} = \text{MCl}_{x-1}^+ \text{RZ} + \text{MCl}_{x+1}^-$	$\text{M} = \text{Al, Zn and Z} = \text{CONH}_2, \text{OH}$

DES types I to III consist of a quaternary ammonium halide complex with a metal chloride, a metal chloride hydrate, and a hydrogen bond donor (HBD), respectively. Type I, can be considered to be of an analogous type to the well-studied metal halide/ imidazolium salt RTIL systems. However, the range of non-hydrated metal halides which have a suitably low melting point to form type I DES is limited. A recent breakthrough suggests that scope of deep eutectic solvents can be widened by replacing non-hydrated metal halides with hydrated metal halides (type II DES). The relatively low cost of many hydrated metal salts coupled with their inherent air/moisture insensitivity makes their use in large scale industrial processes viable.

Type III eutectics, formed from choline chloride and HBD, and it is dominating the current trend of DES research due to their ability to solvate a wide range of transition metal species, including chlorides and oxides [15, 16]. A range of HBD has been studied to date, with DES formed using amides, carboxylic acids, and alcohols (Figure 3). The wide range of HBD available means that this class of deep eutectic solvents is particularly adaptable. The physical properties of the liquid are dependent upon the HBD and can be easily tailored for specific applications. A type IV DES consists of a metal salt combined with a HBD [33].

Unlike RTIL, these liquids are simple to prepare (mixing under moderate heating), and relatively unreactive with water. Most of them are biodegradable and are relatively low in production and material cost. In fact, DES synthesis is 100% atom efficient, solvent-less, and requires no further purification steps, which simplifying scale up. Besides, DES can be made from biodegradable compounds whose toxicology is well characterized and may even include the use of vitamins and metabolites.

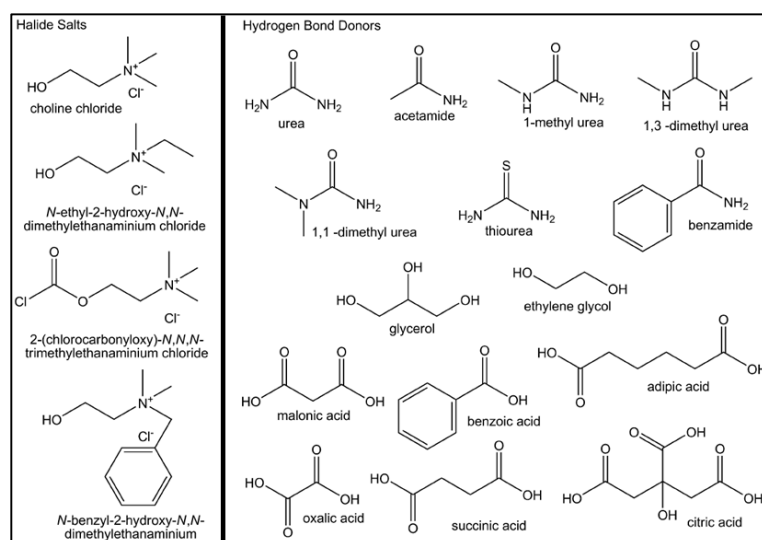


Figure 3. Structures of some halide salts and hydrogen bond donors used in the formation of deep eutectic solvents [31]

2.2 Physical Properties Characterization

2.2.1 Melting Point (MP)

The difference in the MP at the eutectic composition of a binary mixture of A + B is related to the magnitude of the interaction between A and B. The larger the interaction; the larger the difference in MP. In the proper molar ratio, these compounds will form a eutectic with the maximum depression of MP that lies below of their individual compounds. This is shown schematically in Figure 4.

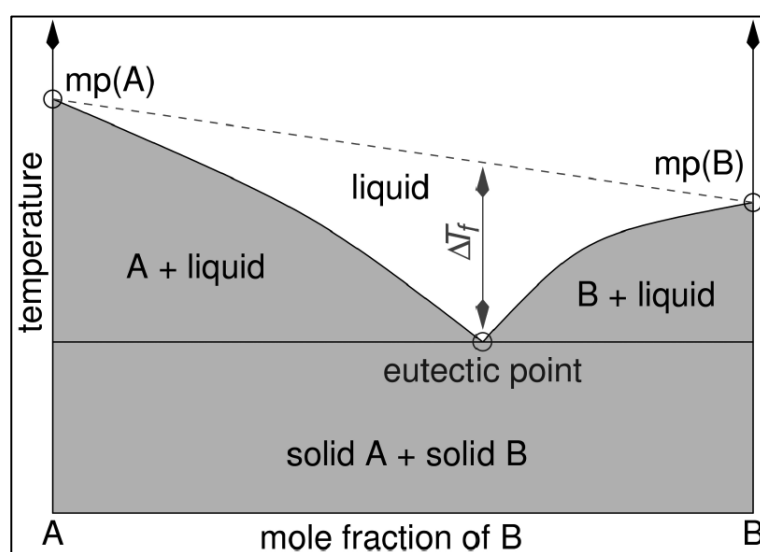


Figure 4. Schematic representation of a eutectic point on a two component phase diagram [31]

In type I eutectics, the interactions between different metal halides and the halide anion from the quaternary ammonium salt will all produce similar halometallate species with similar enthalpies of formation. This suggests that difference in MP values should be between 200 °C and 300 °C. It has been observed that to produce a eutectic at about ambient temperature the metal halide generally needs to have a MP of approximately 300 °C or less. It is evident therefore why metal halides such as AlCl_3 (MP=193 °C), FeCl_3 (MP=308 °C), and ZnCl_2 (MP=290 °C), all produce ambient temperature eutectics. The same is true for quaternary ammonium salts where it is the less symmetrical cations which have a lower MP and therefore lead to lower MP eutectics. This explains why imidazolium halides, C_2mimCl

(mp=87 °C) and C4mimCl (mp=65 °C) have superior phase behaviour and mass transport when compared to ChCl (mp=303 °C).

Type II eutectics are developed to include other metals into the DES family. It is found that metal halide hydrates generally have lower MP than their corresponding anhydrous salt. Waters in hydrated metal salts decrease their MP due to lower lattice energy. As Figure 5 shows, a lower MP of the pure metal salt will produce a smaller depression of MP. Salts with a lower lattice energy will tend to have smaller interactions with the chloride anion. Most of the systems studied yield phase diagrams similar to Figure 4, except for a small number of systems containing AlCl_3 , FeCl_3 , and SnCl_2 which have each shown two eutectic points when mixed with imidazolium chlorides at approximately 33% and 66% metal halide (Figure 6).

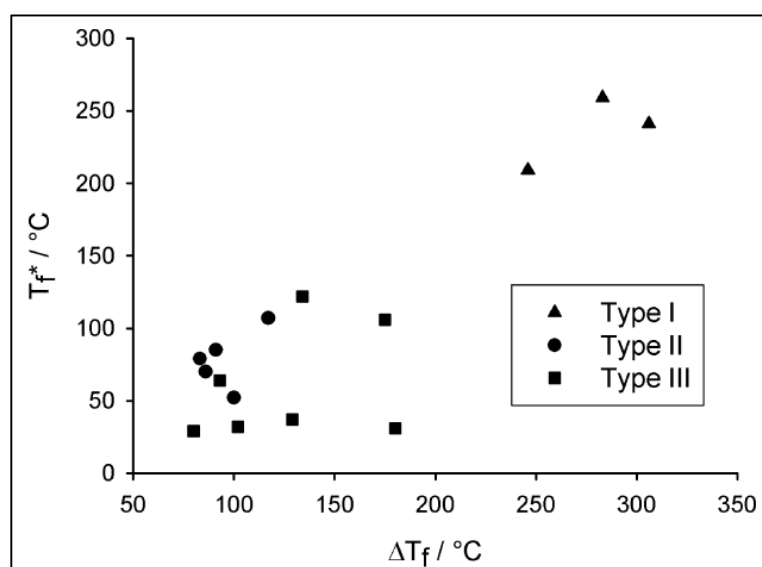


Figure 5. Correlation between the freezing temperature and the depression of freezing point for metal salts and amides when mixed with choline chloride in 2:1 ratio, where the individual points represent different mixture [31]

The type III eutectic mixtures depend upon the formation of hydrogen bonds between the halide anion of the salt and the HBD; where these HBD are multifunctional, the eutectic point tends to be toward a 1:1 or 1:2 molar ratio of salt

and HBD [26]. In the same study the depression of freezing point is shown to be related to the mass fraction of HBD in the mixture.

Table 2. MP of a selection of DES [26, 31, 34]

Salt	MP/ °C	HBD	MP/ °C	Molar Ratio Salt : HBD	DES T_m/ °C
ChCl	303	Urea	134	1:2	12
ChCl	303	Thiourea	175	1:2	69
ChCl	303	1-Methyl Urea	93	1:2	29
ChCl	303	1,3-Dimethyl Urea	102	1:2	70
ChCl	303	1,1-Dimethyl Urea	180	1:2	149
ChCl	303	Acetamide	80	1:2	51
ChCl	303	Benzamide	129	1:2	92
ChCl	303	Adipic Acid	153	1:1	85
ChCl	303	Benzoic Acid	122	1:1	95
ChCl	303	Citric Acid	149	1:1	69
ChCl	303	Malonic Acid	134	1:1	10
ChCl	303	Oxalic Acid	190	1:1	34
ChCl	303	Phenylacetic Acid	77	1:1	25
ChCl	303	Phenylpropionic Acid	48	1:1	20
ChCl	303	Succinic Acid	185	1:1	71
ChCl	303	Tricarballic Acid	159	1:1	90
ChCl	303	MgCl ₂ 6H ₂ O	116	1:1	16

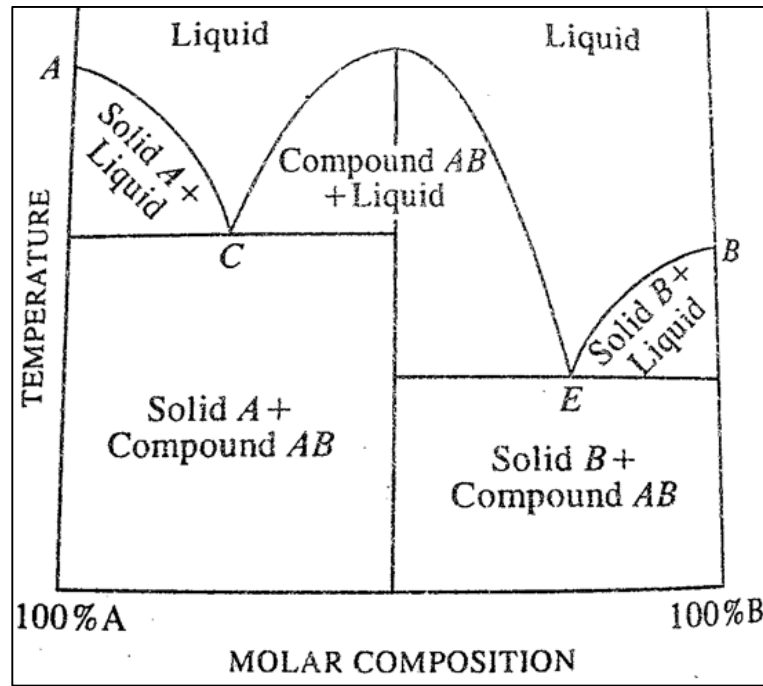


Figure 6. Schematic representation of exceptional cases of two eutectic points on a two component phase diagram [35]

2.2.2 Glass Transition Temperature (T_g)

The glass–liquid transition is the reversible transition in amorphous materials from a hard and relatively brittle state into a molten or rubber–like state [36], which may happen when a viscous liquid is super-cooled into the glass state. Despite the massive change in the physical properties of a material through its glass transition, the transition is not itself a phase transition of any kind; rather it is a laboratory phenomenon extending over a range of temperature and defined by one of several conventions [37]. Such conventions include a constant cooling rate (20 K/min) and a viscosity threshold of 1012 Pa s, among others [36]. Upon cooling or heating through this glass–transition range, the material also exhibits a smooth step in the thermal–expansion coefficient and in the specific heat, with the location of these effects again being dependent on the history of the material [38]. T_g is always lower than the MP, of the crystalline state of the material, if one exists.

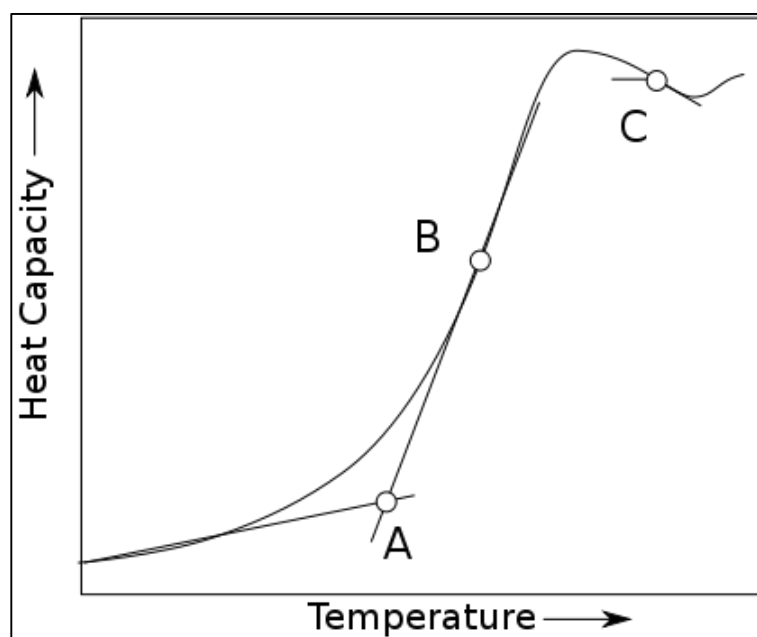


Figure 7. Measurement / Prediction of T_g by DSC

Different operational definitions of T_g are in use, and several of them are endorsed as accepted scientific standards. Nevertheless, all definitions are arbitrary, and all yield different numeric results: at best, values of T_g for a given substance agree within a few kelvins. One definition refers to the viscosity, fixing T_g at a value of 1013 poise (or 1012 Pa s) which is close to the annealing point of many glasses [39]. Another definition involving the use of differential scanning calorimetry (DSC). Figure 7 shows the plotting the heat capacity as a function of temperature. In this context, T_g is the temperature corresponding to point B on the curve. In contrast to viscosity and heat capacity, T_g can too be defined through the relatively sudden change of thermal expansion, shear modulus, and many other properties.

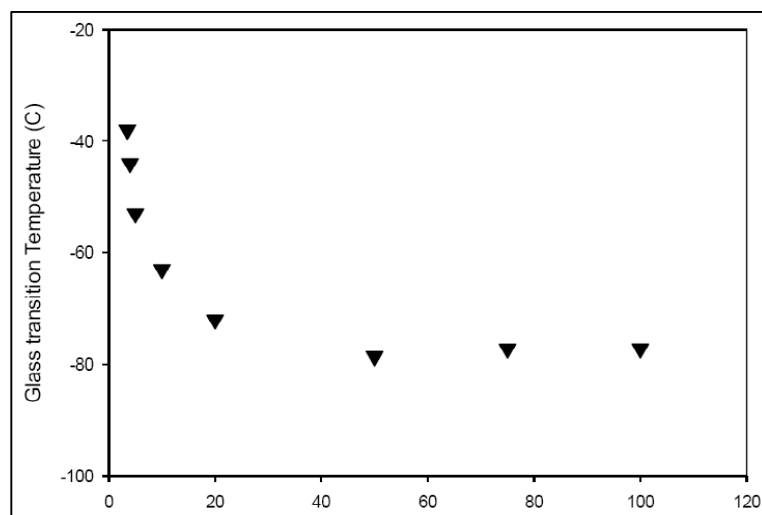


Figure 8. T_g against different molar ratio of Gly observed for the DES between K_2CO_3 and Gly ratios studied in [30]

Practically, T_g shows an increasing trend when concentration of HBD is increase. It can be inferred that higher concentrations of HBD decrease the strength of the hydrogen bonding interactions in the same way as it is postulated for the changes in the viscosity with the HBD concentration. Figure 8 shows DSC curves predicting T_g for different lactic acid: choline chloride based DES ratios. However a different trend is observed in the DES system consists of potassium carbonate (K_2CO_3) and glycerol (GLY). A DES of 1:3.5 molar ratio between K_2CO_3 and glycerol has a T_g -38°C and as the molar ratio glycerol increased, T_g decreased to -78.54°C at 1:50 and almost remained unchanged for the rest of the ratios. This temperature drop is shown Fig. 9 for all DES ratios studied in literature [30].

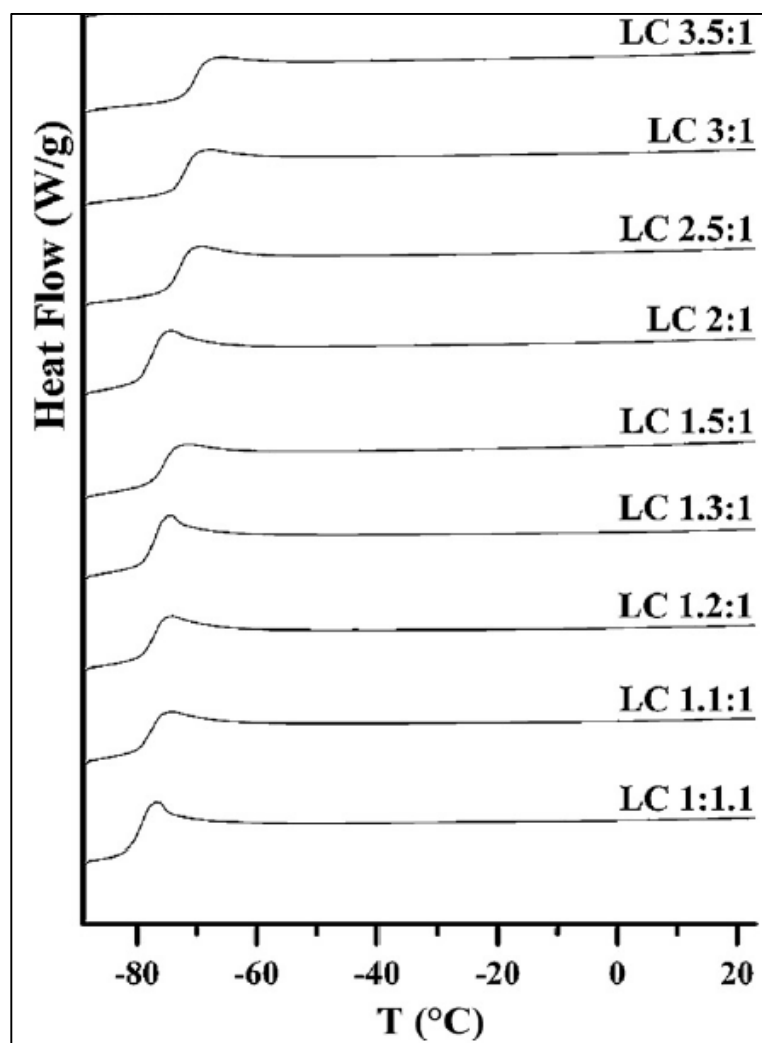


Figure 9. DSC curves showing the trend of T_g for different lactic acid: choline chloride ratios [29]

2.2.3 Density, Viscosity and Refractive Index

Density, viscosity and refractive index are measured as a function of temperature. It is found that the type of salt and HBD and the molar ratio of both compounds had a significant effect on the studied properties [26, 31].

Table 3 shows selected typical physical properties for a variety of DES at the eutectic composition at 298 K. DES is quite high in terms of their viscosity. The origin of this disparity is proposed to be due to the large size of the ions and relatively free volume in the systems.

Table 3. Physical properties of DES at 298K [26, 31]

Halide Salt	HBD	Molar Ratio ChCl: HBD	Viscosity (cP)	Density (g cm ⁻³)
ChCl	Urea	1:2	632	1.24
ChCl	Ethylene Glycol	1:2	36	1.12
ChCl	Glycerol	1:2	376	1.18
ChCl	Malonic Acid	1:1	721	–

In short, density of a DES system can be predicted through the formula

$$\rho_{DES} = \sum_{i=1}^n \rho_i X_i \quad \text{Equation 1}$$

where ρ is density and X_i is the mass fraction of each compounds in the DES systems. A recent study by [40] however concludes that density of DES increased with increasing pressure and decreased with increasing temperature. This phenomenon can be explained through the compressibility and expansibility of DES volumes at different temperature and pressure. The validity of equation can be improve by adding a correction factor as well as a constant, forming a function either of temperature or pressure [41]

$$\rho_T = \rho_0 + m_T T \quad \text{Equation 2}$$

$$\rho_P = \rho_0 + m_P P \quad \text{Equation 3}$$

where ρ is density and m is gradient of linear fitted line using least-squares method on experimental data.

Overall, density of DES is represented as a function of temperature and pressure by a Tait-type equation of the form [40]

$$\rho(T, P) = \frac{\rho_o(T)}{1 - C \ln(B(T) + \frac{P}{B(T)} + P_{ref})} \quad \text{Equation 4}$$

where ρ_o is the reference density; P_{ref} is the reference pressure (0.1 MPa); and C , $B(T)$ are adjustable parameters determined by fitting the data into equation above by

applying the Marquardt method. The parameter C is assumed to be independent of temperature while B is assumed to be temperature-dependent.

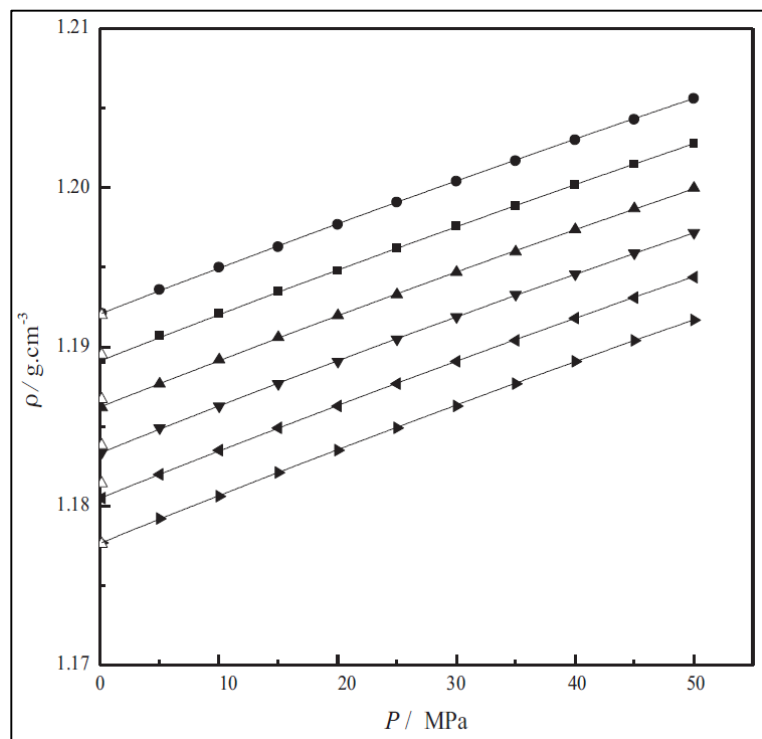


Figure 10. Density of ChCl: Gly (1:2) as a function of pressure at different temperatures: ●, 298.15 K; ■, 303.15 K; ▲, 308.15 K; ▼, 313.15 K; ◄, 318.15 K; ►, 323.15 K [40]

For viscosity, the same trend of decreasing viscosity with increasing temperature is observed. Research conducted by [42] shows that DES is non-Newtonian fluids and they are shear thinning or thixotropic in properties (Figure 11).

At low temperature, the difference in viscosity observed for different molar ratio are significant. However, at high temperature, viscosity of DES at different molar mixing ratio are found to be converged to one point (Figure 12 and Figure 13).

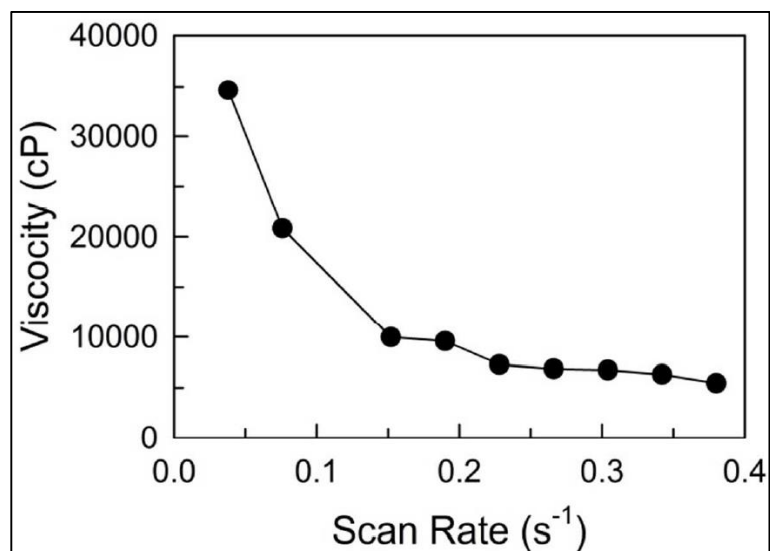


Figure 11. Shear rate–dependent viscosity of 1:2:6 ChCl: Gly: 1,5-Diazabicyclo[4.3.0]non-5-ene (DBN) measured at 298.15K [42]

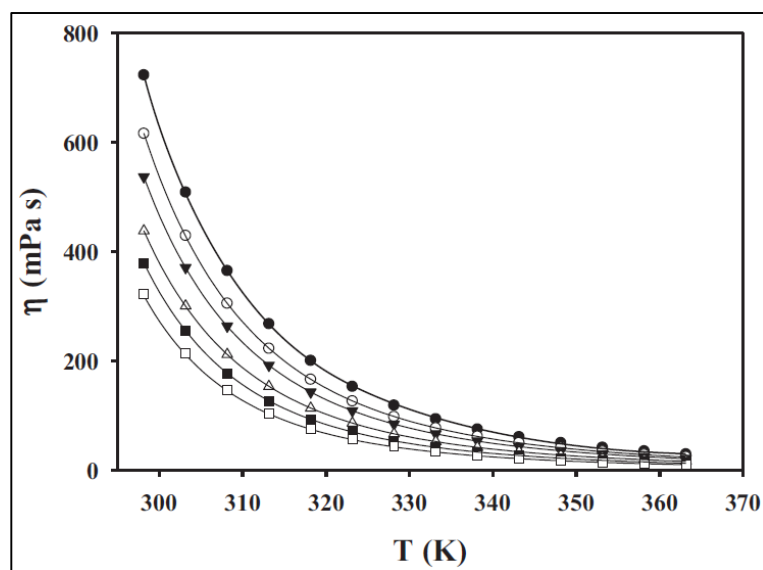


Figure 12. Viscosity change with temperature for lactic acid: choline chloride LTTM at different molar ratios: ●, 1.3:1; ○, 1.5:1; ▼, 2:1; △, 3:1; ■, 5:1; □, 10:1 [29]

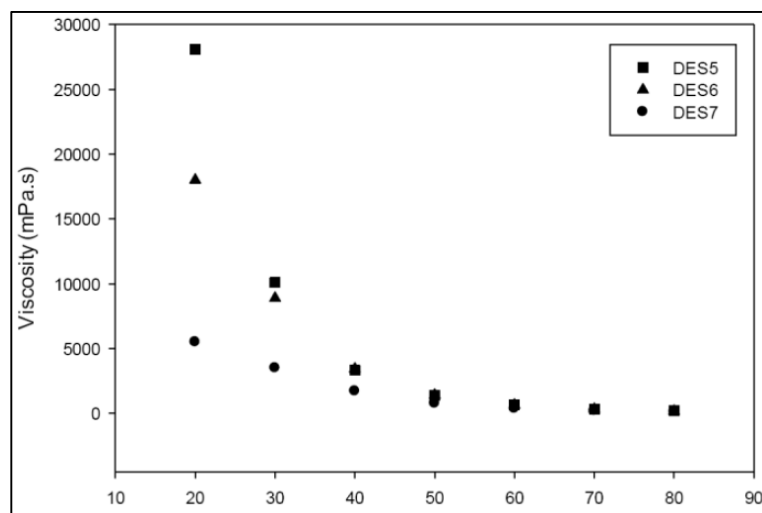


Figure 13. Dynamic viscosity of selected DES containing K_2CO_3 and Gly (1:4, 1:5, 1:6) as function of temperature [30]

According to [41], refractive index (RI) could be important as it might provide important information on the purity of samples and molecular interaction in the liquid. For pure DES, RI is found to be decrease linearly with temperature. Similar with density, RI can be correlates with temperature using linear estimation of functions.

$$n_T = n_0 + m_T T \quad \text{Equation 5}$$

where n is RI and m is gradient of linear fitted line using least-squares method on experimental data. Table 4 shows the RI of ChCl: ethylene glycol (Eth) and ChCl: glycerol DES.

Table 4. RI of ChCl: ethylene glycol (Eth) and ChCl: Gly DES [41]

T (K)	RI	
	ChCl: Ethylene Glycol	ChCl: Glycerol
298.15	1.46823	1.48675
303.15	1.46699	1.48558
308.15	1.46575	1.48443
313.15	1.46445	1.48326
318.15	1.46320	1.48211
323.15	1.46197	1.48093

328.15	1.46078	1.47978
333.15	1.45954	1.47856

Surface tension could be expected to follow similar trends to viscosity since it is a measure of how strong the intermolecular forces are in the liquid, similar to the measure of viscosity. It is reasonable to expect that as viscosity increases with an increase in the molar composition of ChCl, the surface tension should increase as the molar composition of ChCl increases [43]. A plot of surface tension as a function of temperature can be seen in Figure 14.

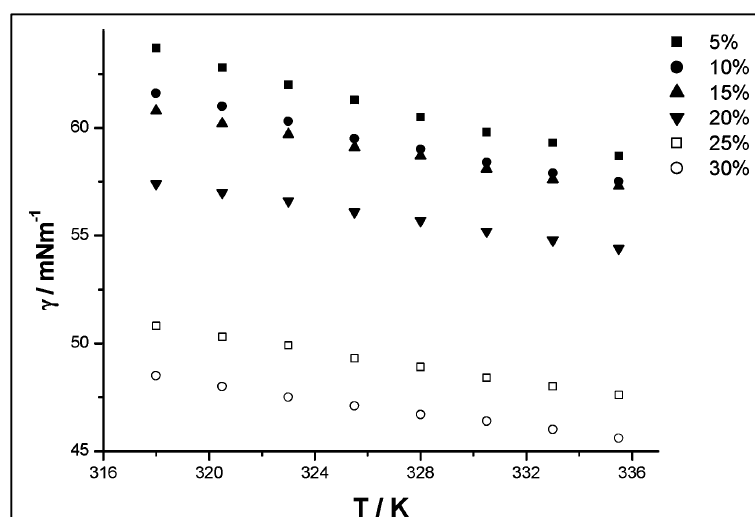


Figure 14. Plot of temperature versus surface tension for different concentration of glycerol in DES [43]

2.3 Material Selection

2.3.1 Choline Chloride (ChCl)

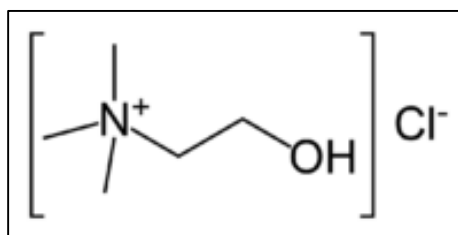


Figure 15. IUPAC structure of ChCl [44]

The most studied DES perhaps is based on ChCl (also known as (2-hydroxyethyl) trimethylammonium chloride). ChCl is the quaternary ammonium salt which is non-toxic, biodegradable, and relatively cheaper. Choline cation belongs to an important class of vitamin B family and it is considered to play an essential role in our daily life by assisting in various metabolic mechanisms [18, 19]. ChCl also mass produced to serves as a nutritional supplement of animal feedstock [20, 21].

Table 5. Properties of ChCl [44]

Molecular formula	C ₅ H ₁₄ ClNO
Molar mass	139.62 g/mol
Appearance	White or deliquescent crystals
Melting point	302 °C (576 °F; 575 K) (decomposes)
Solubility in water	very soluble (>650 g/l)

2.3.2 Glycerol (Gly)

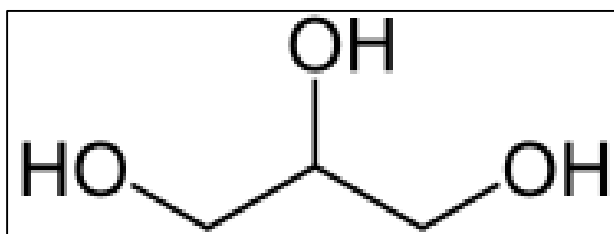


Figure 16. IUPAC structure of Gly [44]

Gly (1, 2, 3-propanetriol) is a non-toxic, colourless, odourless, viscous liquid with a sweet taste, derived from both natural and petrochemical feedstock. The name glycerol is derived from the Greek word for sweet (glykys), and the terms glycerin, glycerine, and glycerol tend to be used interchangeably in the literature [30]. In its pure form, Glycerol has 1.261 specific gravity, 1500 cP viscosity, 64 dyne/cm surface tension (all at 293.15 K) and a freezing point of 18.2 °C [44]. In DES, Glycerol has been successfully used as a HBD with Choline Chloride to form DES by several research groups [33, 40-43, 45, 46].

Table 6. Properties of Glycerol [44]

Molecular formula	C ₃ H ₈ O
Molar mass	139.62 g/mol
Appearance	colourless liquid, hygroscopic
Melting point	17.8 °C (64.0 °F; 290.9 K)
Refractive Index	1.4746 at 25 °C

2.3.3 L-Arginine (L-Arg)

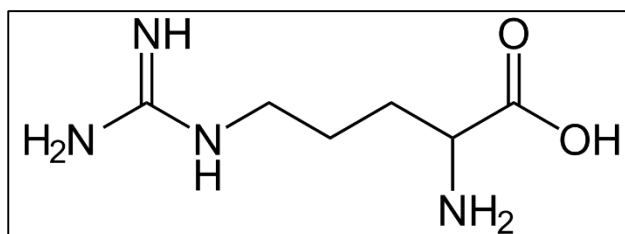


Figure 17. IUPAC structure of L-Arg in its un-ionized form

L-Arg is an α -amino acid which is first isolated in 1886 [47]. Amino acids are biologically important organic compounds composed of amine ($-\text{NH}_2$) and carboxylic acid ($-\text{COOH}$) functional groups, along with a side-chain specific to each amino acid. The key elements of an amino acid are carbon, hydrogen, oxygen, and nitrogen. It can be assorted base on their structure and the general chemical characteristics of their functional groups (Figure 19). Table 7 compares the properties among 21 common amino acids for the selection of suitable ternary component. Among factors that take into consideration includes:

- Non-complex compound [42]
- Basic polar side chain [30, 42]

Table 7 shows the side chain polarity and charge of common amino acids with their hydropathy index. L-ARG consists of a 3-carbon aliphatic straight chain, the distal end of which is capped by a complex guanidinium group. Since it is proven that

basic polar compounds will enhance the absorbance of CO₂, L-Arg is prioritized in this study for their basic polar side chain and high resultant pK_a value (12.48) [30, 42]. The guanidinium group of L-Arg is positively charged in neutral, acidic, and even most basic environments, and thus imparts basic chemical properties to arginine. Because of the conjugation between the double bond and the nitrogen lone pairs, the positive charge is delocalized, enabling the formation of multiple H-bonds (Figure 18).

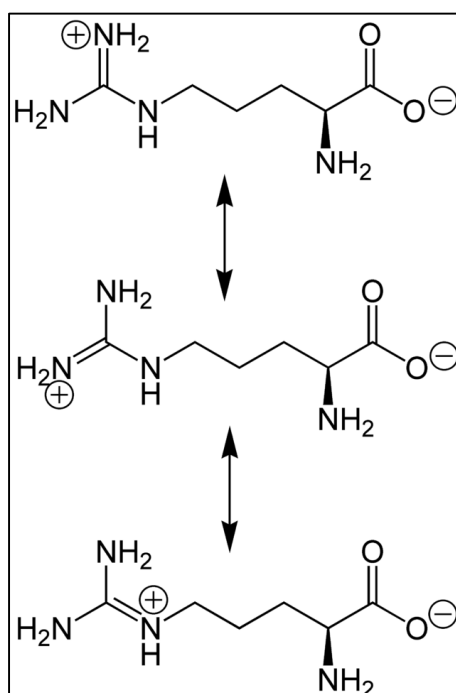


Figure 18. Delocalization of charge in guanidinium group of L-Arg [48]

Table 7. Properties of common amino acids with polar side chain [48]

Amino Acid	Side Chain	Side-Chain Polarity	pK _a	Hydropathy Index
Arginine	$-(\text{CH}_2)_3\text{NH}-\text{C}(\text{NH})\text{NH}_2$	Basic Polar	12.48	-4.5
Lysine	$-(\text{CH}_2)_4\text{NH}_2$	Basic Polar	10.54	-3.9
Histidine	$-\text{CH}_2-\text{C}_3\text{H}_3\text{N}_2$	Basic Polar	6.04	-3.2
Serine	$-\text{CH}_2\text{OH}$	Polar	5.68	-0.8
Threonine	$-\text{CH}_2\text{C}_3\text{H}_6\text{N}$	Polar	5.89	-0.7
Tyrosine	$-\text{CH}_2-\text{C}_6\text{H}_4\text{OH}$	Polar	10.46	-1.3

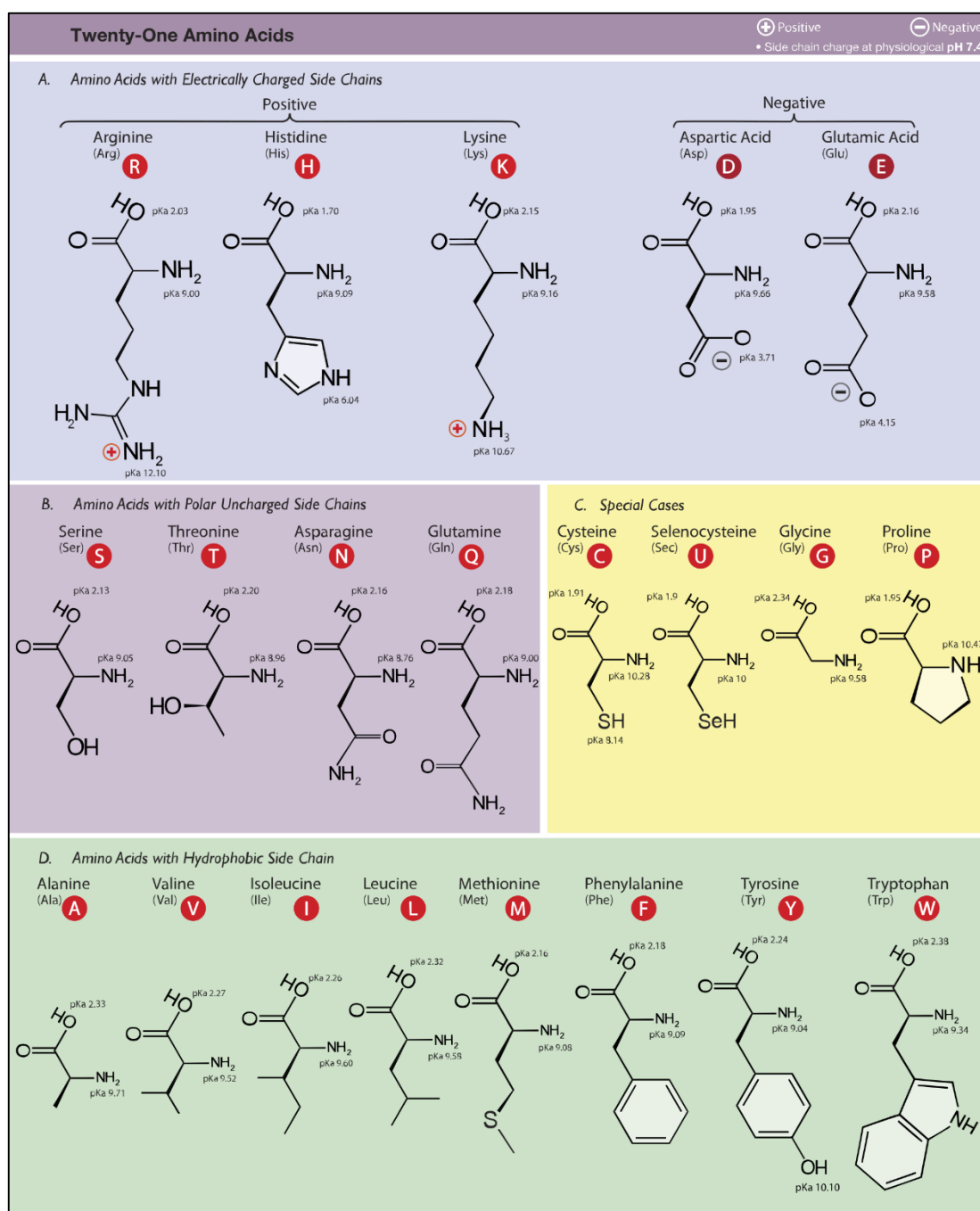


Figure 19. Grouped table of 21 amino acids' structures, nomenclature, and their side groups' pKa values [48]

CHAPTER 3

METHODOLOGY/PROJECT WORK

3.1 Materials and Apparatus

Analytical grade of ChCl, Gly, and L-Arg are purchased from Merck Chemicals and Sigma–Aldrich Chemicals and used as received without further purification. The equipment related to the project and their roles are as in Table 8.

Table 8. Equipment list for the project

Equipment	Model	Function	Location
Hot Magnetic Stirring Plate	-	Heating and mixing	Block 05-01-05
Drying Oven	Mettler	Drying of chemicals before mixing	Block 05-01-05
Vacuum Oven	Mettler	Moisture removal from DES / LTTM	Block 03-02-03
Thermal Gravimetry Analyzer	Perkin Elmer STA6000	Evaluate the thermal stability of DES	Block 04-01-06
Differential Scanning Calorimetry	Mettler Toledo DSC1	Evaluate the melting point or glass transition temperature of DES	Block 04-01-06
Karl Fischer Coulometer	Mettler Toledo DL39	Determine the water content of resulted DES	Block 04-01-06
Density Meter	Anton Paar	Observe the changes of density at	Block N

	DMA 4500M	different temperature	
Viscometer	Anton Paar LOVIS 2000M	Determine the viscosity of DES at different temperature and shear rate	Block N
Refractive Index	Atago RX– 5000α	Study the changes of refractive index at different temperature	Block 03-00-06

3.2 Methodology

In this research, novel DES / LTTM has been synthesized and characterized. The prepared DES / LTTM is chosen based on the structure of salts and the HBD.

3.2.1 Synthesis of LTTM System

In order to prepare our DES / LTTM mixtures, a binary DES mixture of ChCl and Gly is first prepared by mixing ChCl and Gly in the appropriate molar ratio under vigorous stirring at 80 °C for 30 minutes. Stirring is continued for another hour without heating allowing the mixture to cool to room temperature. The resulting solutions are clear and homogeneous. Then, the LTTM of ChCl, Gly and ternary component is subsequently prepared by heating the binary DES to 80 °C followed by addition of appropriate mass of the ternary component while stirring. The final mixture is then stirred for up to 2 hours to ensure homogeneity of resultant LTTM before allowing it to cool to ambient temperature. The solution is left overnight at room temperature to ensure no precipitation of ternary component occurred. After that, the solvent is dried at 85 °C under 500 mBar of vacuum for 48 hours. At this point, the LTTM is ready for use. It is important to note that no purification step is required and no additional solvents are employed in the preparation of this LTTM.

3.2.2 Characterization of LTTM

The DES will be characterized by studying physicochemical properties (i.e. density, viscosity, refractive index, melting point, thermal gravimetric analysis (TGA),

differential scanning calorimeter (DSC) etc.) over temperature range of 293.15 K up to 343.15 K at atmospheric pressure for the whole range of composition.

3.3 Project Feasibility

This project is allocated around five months to be completed. It is expected that there will be ample time to complete the project objectives. Parameters are carefully chosen to suit the timeline for the project. Besides, a reasonable and detailed planning has been devised for each part of the project, this is so that the project can be completed within the planned timeframe and will produce a good outcome by the end.

3.4 Gantt Chart and Key Milestones

The Gantt chart is as Table 14, and key milestones are starred.

Table 9. Gantt chart with key milestones

Task / Week	FYP I														FYP II											
	1	2	3	4	5	6	7	8	9	10	11	12	13	14	1	2	3	4	5	6	7	8	9	10	11	12
Introduction to FYP																										
Meeting with Supervisor																										
Literature Review / Methodology																										
Procurement of workspace, chemicals and equipment																										
Submission of Extended Proposal																										
Proposal Defence																										
Synthesis of DES																										
Characterization of DES																										
Determination of DES optimum molar mixing ratio																										
Submission of Interim Report																										

CHAPTER 4

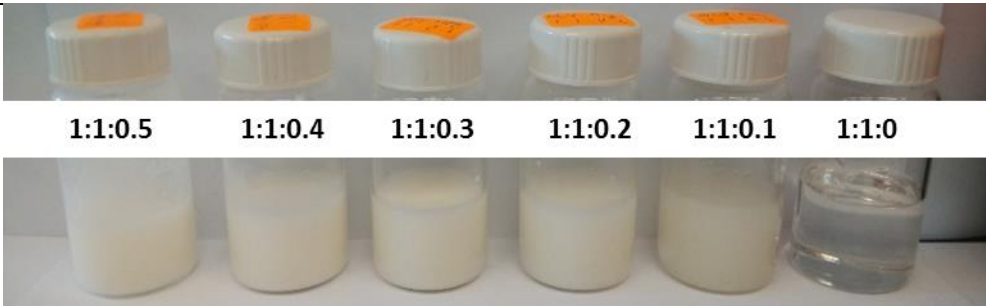
RESULT AND DISCUSSION

4.1 Formation of Solvents

From previous study, different ratio of glyceline are mixed at ratio of 1:1, 1:2, 1:3, 1:4, 1:6 and 1:8. In this study, arginine is added into these system at different ratio to determine the maximum ratio of arginine that is able to react with glyceline through hydrogen bonding and form clear eutectic solvent (Table 10).

From Tsable 10, it can be clearly seen that arginine only form eutectics with glyceline at glyceline ratio of 1:2 and above. The criteria of selecting feasible eutectic solvents includes, the solvent is clear at the end of mixing, liquid phase at room temperature (20 °C), less than 120 mins of mixing time at 80 °C under 350 rpm of stirring and no recrystallization of solids after the resultant solvent is sealed air tight and left untouched for 12hour.

Table 10. Eutectic solvents formed with arginine and glyceline of different ratio

glyceline Ratio	
1:1	
	1:1:0.5 1:1:0.4 1:1:0.3 1:1:0.2 1:1:0.1 1:1:0

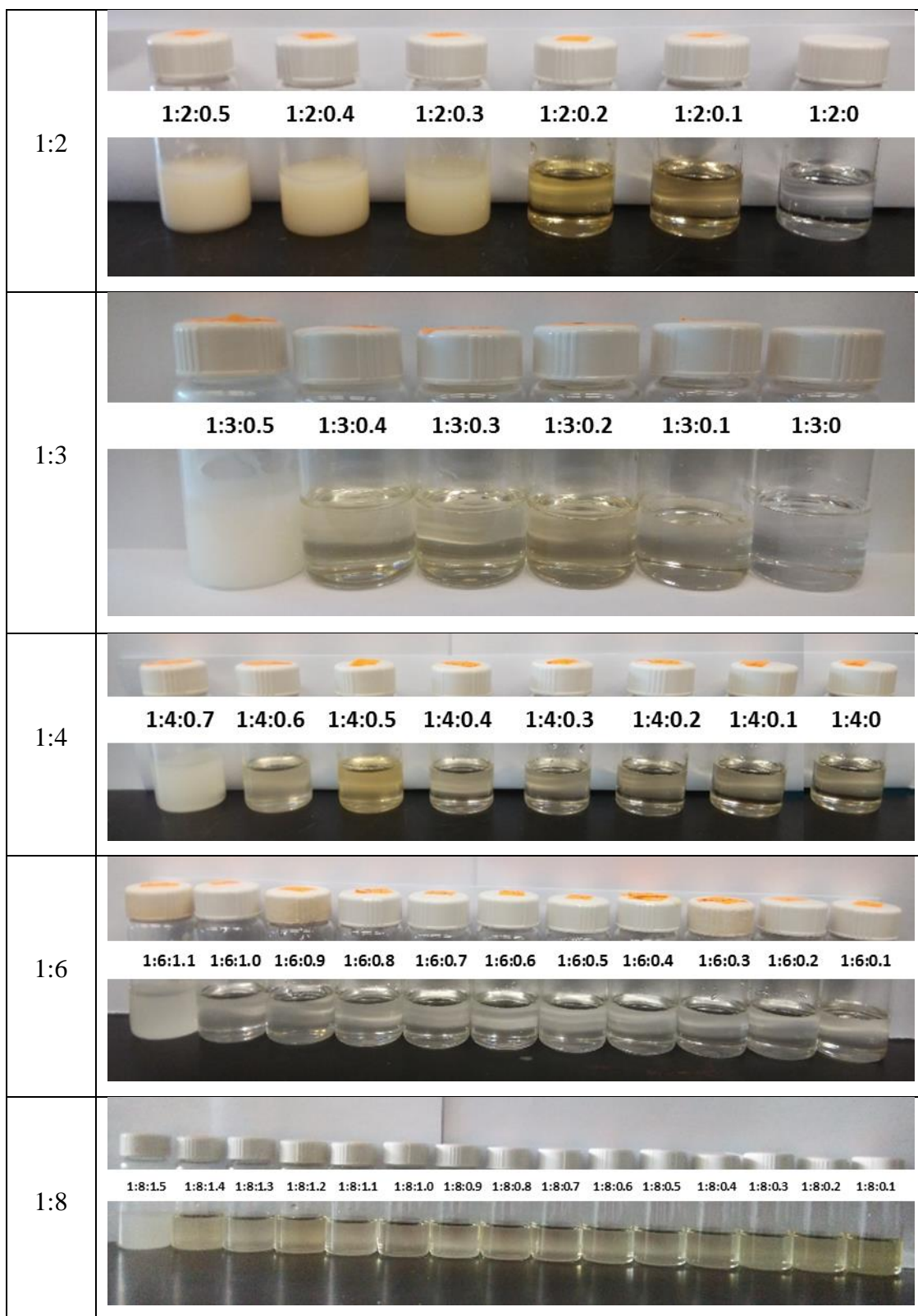


Figure 20 shows the graph of maximum molar ratio of arginine against molar ratio of glycerol in the glycine system. The maximum molar ratio of arginine that can

form feasible eutectics with glycerol from the experimental data is expressed through the following equation

$$R_{Arginine} = 0.2 R_{Glycerol} - 0.2 \quad \text{Equation 6}$$

Here, $R_{Arginine}$ and $R_{Glycerol}$ refer to molar ratio of the components in the ternary deep eutectic solvent system. From the preliminary mixing, it can be deduced that arginine is participating the hydrogen bonding as salt or hydrogen bond acceptor since it can form eutectics with excess hydrogen bond donor, glycerol for glyceline with ratio 1:2 and above but not with lower ratio (ie. glyceline 1:1). Although glyceline 1:2 is defined by previous research as the eutectic point of the binary mixture between choline chloride and glycerol, the experiment however shows that the system is not saturated, 0.2 mol ratio of arginine is still able to have hydrogen bonding interaction with the currently saturated system as defined by previous research [31, 43, 49].

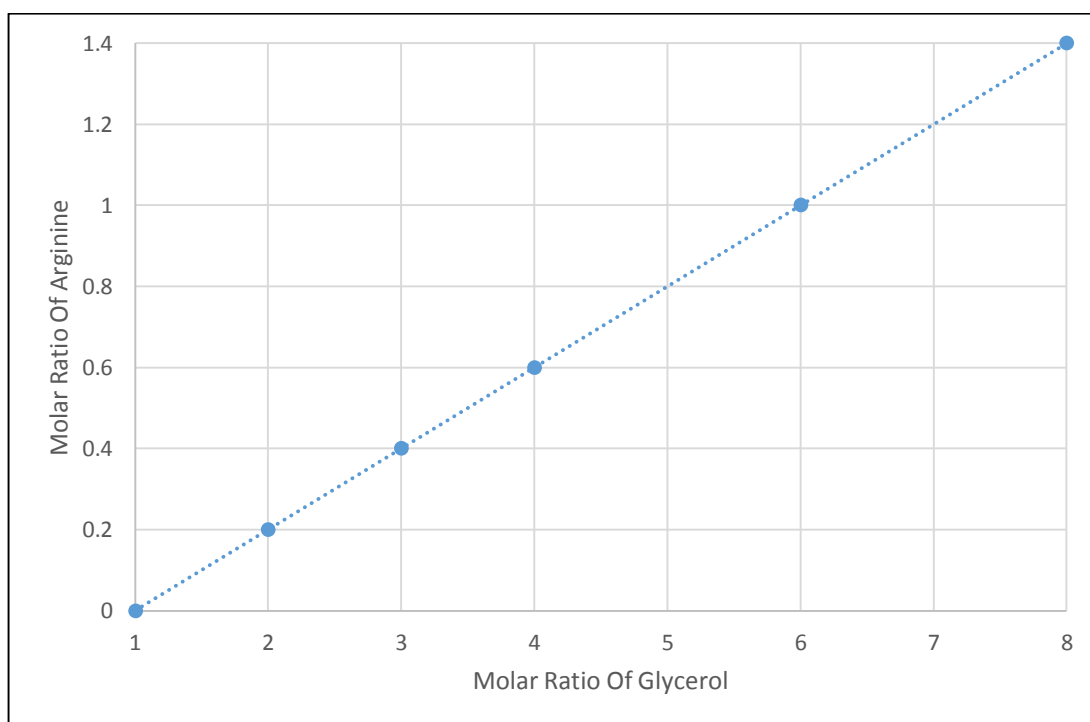


Figure 20. Graph of molar ratio of arginine against molar ratio of glycerol

Glyceline 1:2, 1:3 and 1:4 are used in the study as they are commonly used in research for characterization. Molar ratio of arginine added into system are up to 0.2 only, although higher ratio of glycerol (Gly) can accommodate more L-Arginine (L-Arg), the higher the molar ratio of Gly and L-Arg present in the system, the eutectics

formed is more viscous. For the characterization process, glyceline consisting different ratios of choline chloride (ChCl) and Gly are mixed as in Table 11.

Table 11. Mass of individual component of glyceline for mixing

Abbreviation	Mass		Mol		Mol Ratio	
	ChCl	Gly	ChCl	Gly	ChCl	Gly
DES 1	45.270	59.737	0.324	0.649	1	2.0004
DES 2	35.278	69.825	0.253	0.758	1	3.0005
DES 3	29.059	76.763	0.208	0.833	1	4.0046

LTTM consisting different ratio of glyceline and amino acids (L-Arg) is mixed as specified in Table 12.

Table 12. Mass of individual component of LTTM for mixing

Abbreviation	Mass		Mol		Mol Ratio	
	glyceline	Arg	glyceline	Arg	glyceline	Arg
DES 4	9.493	0.511	0.029 : 0.059	0.003	1 : 2.0004	0.1001
DES 5	9.262	0.993	0.029 : 0.057	0.006	1 : 2.0004	0.1993
DES 6	9.604	0.401	0.023 : 0.069	0.002	1 : 3.0005	0.0997
DES 7	9.230	0.773	0.022 : 0.067	0.004	1 : 3.0005	0.2000
DES 8	9.672	0.355	0.019 : 0.076	0.002	1 : 4.0046	0.1071
DES 9	9.357	0.641	0.018 : 0.074	0.004	1 : 4.0046	0.1999

4.2 Water Content

Glyceline is a hygroscopic eutectics where it tends to absorb moisture in air when expose to the environment. Therefore, as an effort to reduce the error and deviations in characterization process, the samples are dried in vacuum oven at 500mBar and 85 °C to remove as much moisture as possible. The water content of samples after drying is determined using Karl Fischer titration and is presented in table 13.

Table 13. Water content of DES

Abbreviation	DES	Water Content (wt%)
DES 1	1 : 2	1.07
DES 2	1 : 3	1.90
DES 3	1 : 4	1.28
DES 4	1 : 2 : 0.1	1.46
DES 5	1 : 2 : 0.2	1.76
DES 6	1 : 3 : 0.1	2.13
DES 7	1 : 3 : 0.2	2.36
DES 8	1 : 4 : 0.1	1.13
DES 9	1 : 4 : 0.2	1.27

4.3 Thermal Properties

4.3.1 Decomposition Temperature

Thermal gravimetric analysis (TGA) is conducted on all binary and ternary DES / LTTM to evaluate the thermal stability by means of determining the degradation temperature. The accuracy of TGA result in determining the decomposition temperature of DES can be influenced by various operating parameters and condition, such as heating rate, temperature, pressure, moisture content, and composition of sample. The DES samples are heated up to 673.15K from room temperature at a scanning rate of 5K.min⁻¹ under continuous nitrogen flow of 20mL.min⁻¹ to avoid oxidation of samples. The resolution of result is greatly dependant on the scanning rate where the lower the ramp, the higher the resolution. Moreover, higher heating rate may result in slight changes in TGA curve, showing a higher decomposition temperature [50, 51]. Under the above-mentioned operating conditions, the thermal stability of DES is studied at the intersection of extrapolated constant mass and the slope of the mass loss at inflection point. Results are presented in Table 14 and in Figures 21.

As observed in Table 14, the decomposition temperature of DES / LTTM decreased with arginine added into the system. Among all the binary DES, glyceline 1:2 ratio is

having the highest thermal stability and decomposition temperature. Overall, as the glycerol and arginine content in DES / LTTM increased, the thermal stability of DES is reduced.

For glyceline 1:2, as arginine content in the DES increased, decomposition temperature of DES decrease. This may be due to addition of arginine is disrupting the saturated strong hydrogen bonding between choline chloride and glycerol in the glyceline system as arginine contains positively charged guanidinium group (pKa 12.48). It is possible that when guanidinium group of arginine is delocalized, it tends to form stronger ionic-like bonding with the chloride of choline chloride, allowing the amine group and other parts of arginine to form hydrogen bonding with glycerol substituting the role of chloride.

Although similar trend is observed in other glyceline system, there are some exceptions. When 0.2 molar ratio is added into glyceline 1:4, the decomposition temperature of DES increased, up to decomposition temperature of glyceline 1:4. This phenomenon can be explained through hydrogen bonding and eutectic ratio. Theoretically, when eutectic ratio in DES is achieved, all the components in DES will be bonded through strong hydrogen bonding and increment of decomposition temperature or high depression of melting temperature will be observed. The increment of thermal stability suggest that 0.2 molar ratio of arginine are forming strong hydrogen bond with the free glycerol in glyceline 1:4 system.

The decomposition temperature of glyceline 1:2 is compared with previous paper and the Average absolute deviation percentage (AAD%) is calculated based on equation to report error of experimental data against reference data.

$$AAD\% = \left(\frac{100}{n}\right) \sum_{i=1}^n \left(\frac{|D_{literature} - D_{experimental}|}{D_{experimental}}\right) \quad \text{Equation 7}$$

where D and n is data and number of measurement respectively. The AAD% found is 0.945% which the reliability of the data obtained is high.

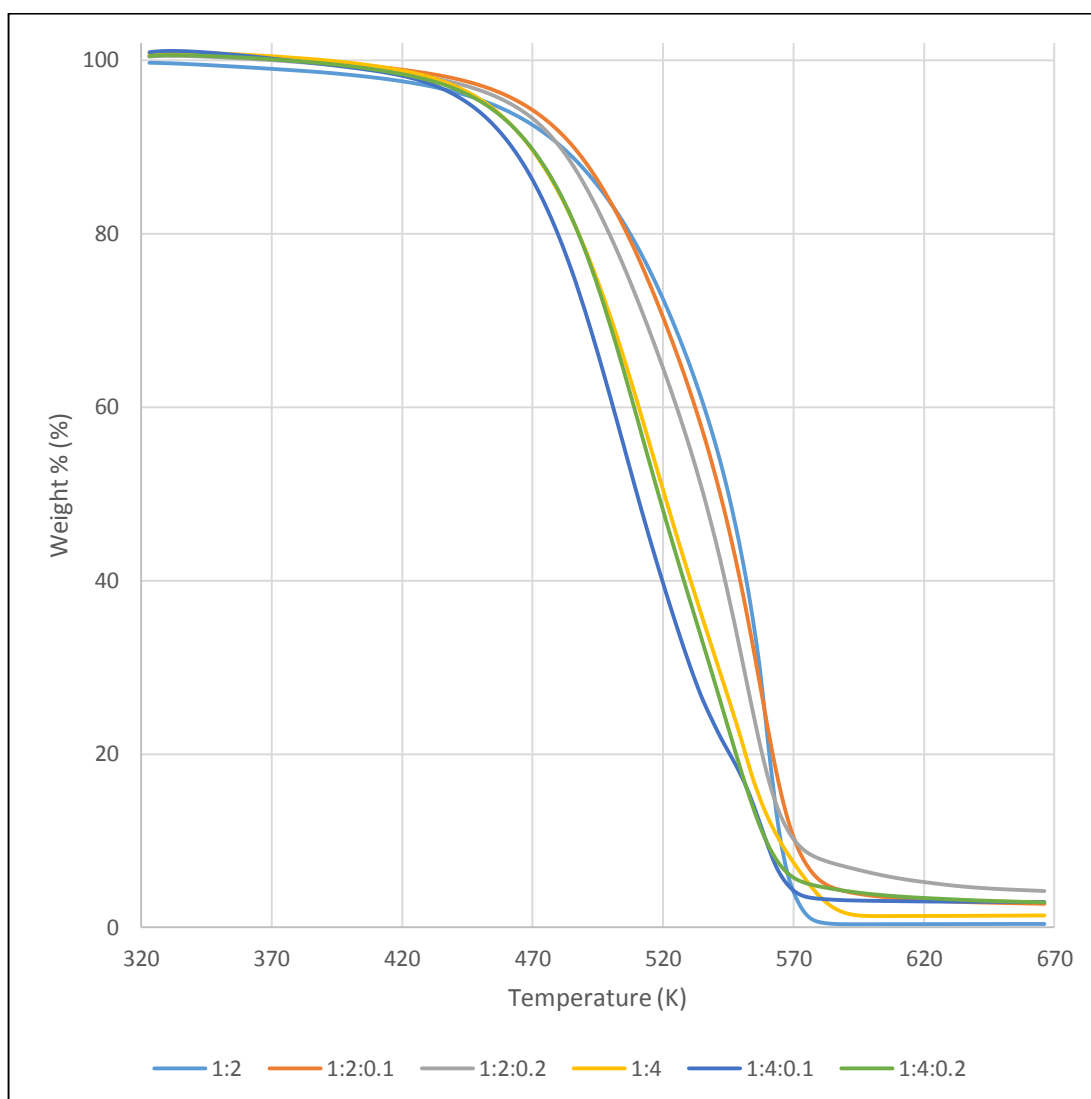


Figure 21. TGA curves of DES / LTTM

Table 14. Decomposition temperature data of DES

Abbreviation	DES	T _{decomposition} (K)	T _{decomposition} (K) (lit.)
DES 1	1 : 2	528.11	533.15 ^a
DES 2	1 : 3	513.81	-
DES 3	1 : 4	472.31	-
DES 4	1 : 2 : 0.1	514.1	-
DES 5	1 : 2 : 0.2	502.69	-
DES 6	1 : 3 : 0.1	502.68	-

DES 7	1 : 3 : 0.2	486.82	-
DES 8	1 : 4 : 0.1	465.42	-
DES 9	1 : 4 : 0.2	472.07	-

^aRef. [52]

4.3.2 Melting Point / Glass Transition Temperature (MP / T_g)

Differential scanning calorimetry (DSC) is conducted on all binary and ternary DES / LTTM to determine the MP / T_g of DES / LTTM. The MP / T_g is measured based on changes of amount of heat required to increase the temperature of a sample and reference which are measured as a function of temperature. The accuracy of DSC result in determining the MP / T_g of DES / LTTM can be influenced by various operating parameters and condition, such as heating rate, temperature, pressure, moisture content, and composition of sample.

The DES / LTTM samples are first heated up to 403.15K from room temperature at a scanning rate of 10K.min⁻¹ under continuous nitrogen flow of 20mL.min⁻¹ to avoid oxidation of samples, then it is cooled down to 123.15K at a scanning rate of 10K.min⁻¹ under continuous nitrogen flow of 20mL.min⁻¹, before reheat it up to 403.15K again at a scanning rate of 10K.min⁻¹ under continuous nitrogen flow of 20mL.min⁻¹. The scanning program is portrayed in Figure 22. The resolution of result is greatly dependant on the scanning rate where the lower the ramp, the higher the resolution. Under the above-mentioned operating conditions and scanning program, the MP / T_g of DES / LTTM is studied at the intersection of extrapolated constant mass and the slope of the mass loss at inflection point. Results are presented in Table 15 and in Figures 23.

From the result as shown in Table 15, all DES / LTTM does not shows their melting point, instead, glass transition with enthalpy relaxation is observed for each DES / LTTM. Therefore, the resultant solvents are categorized under LTTM rather than DES.

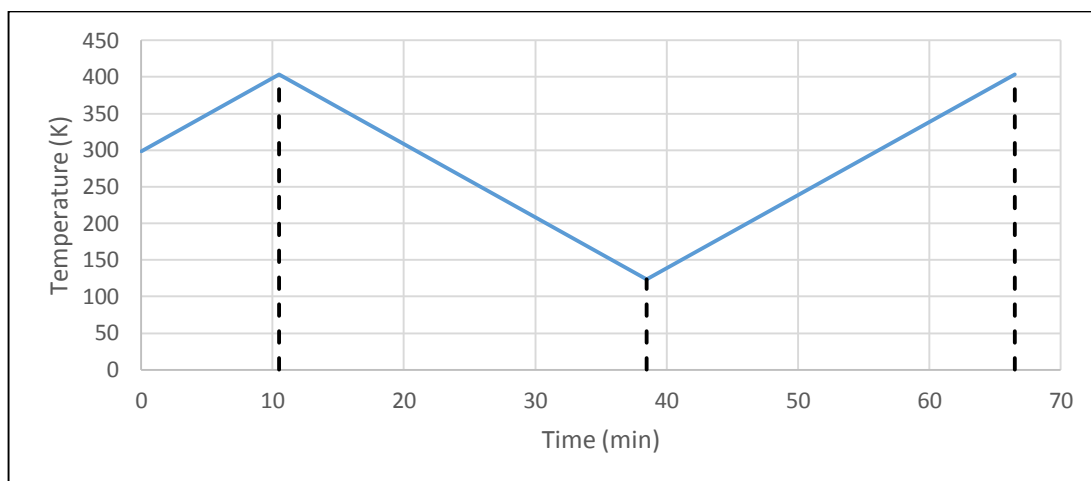


Figure 22. DES scanning program for all DES / LTTM

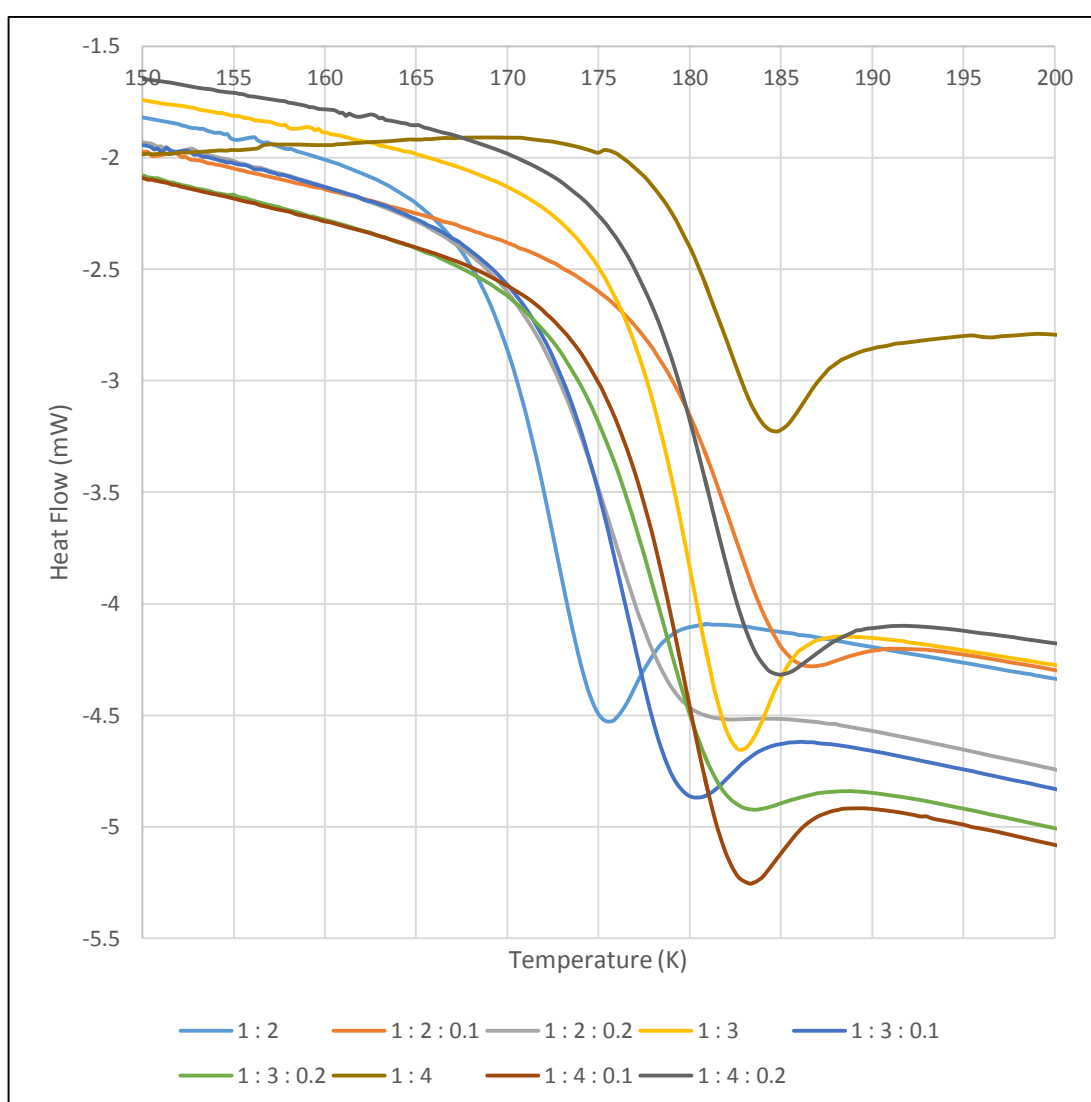


Figure 23. DSC curves of DES / LTTM

4.4 Physical Properties

4.4.1 Density

The density of all DES / LTTM is measured as a function of temperature and are depicted in Figure 24 and Table 16 to 18. All raw data of experimentally determined values can be found in Appendix. The AAD% of the experimental data is found to range from 0.170% to 0.665% with an average of 0.339%. As observed from Figure, the density increased linearly with increasing temperature. The density of binary DES increased with increasing molar ratio of glycerol and the density of ternary DES increased with the increment addition of L-arginine. This is justifiable since the density of Gly and L-Arg are 1.26g/cm³ and 1.3g/cm³ respectively at STP. The dotted lines in figure 24 show that density of DES can be fitted with linear fit in the form of equation 8. The fitting parameters which are m and c based on equation 8 are available in Table 19.

$$\rho = mT + c \quad \text{Equation 8}$$

Where ρ is density of DES, T is temperature in Kelvin while m and c are the fitting parameters varied for different binary and ternary DES. Table shows the fitting parameters of density of each DES.

Table 15. Density versus temperature data for DES (1:2, 1:2 (lit.), 1:2:0.1 and 1:2:0.2) over the temperature range (298.15-343.15) K

T/K	1 : 2	1 : 2 (lit.)	1 : 2 : 0.1	1 : 2 : 0.2
298.15	1.18785	1.18 ^{a, f} 1.1921 ^b 1.19123 ^d	1.19455	1.19985
303.15	1.18507	1.1892 ^b 1.1895 ^c 1.1885 ^{d, e}	1.19181	1.19705
308.15	1.18228	1.1862 ^b 1.18574 ^d	1.18906	1.19431
313.15	1.17949	1.1834 ^b 1.1838 ^c	1.18631	1.19158

		1.1823 ^d 1.1827 ^e		
318.15	1.17670	1.1805 ^b 1.18022 ^d	1.18355	1.18884
323.15	1.17391	1.1777 ^b 1.1776 ^c 1.17746 ^d 1.1770 ^e	1.18078	1.18610
328.15	1.17113	1.17468 ^d	1.17801	1.18334
333.15	1.16836	1.1741 ^c 1.17193 ^d 1.1713 ^e	1.17525	1.18059
338.15	1.16559	-	1.17250	1.17784
343.15	1.16282	1.1674 ^c 1.1648 ^e	1.16976	1.17509

Measurement are performed at atmospheric pressure. ^aRef. [31], ^bRef. [40], ^cRef. [53], ^dRef. [41], ^eRef. [33], ^fRef. [49]

Table 16. Density versus temperature data for DES (1:3, 1:3:0.1 and 1:3:0.2) over the temperature range (298.15-343.15) K

T/K	1 : 3	1 : 3 : 0.1	1 : 3 : 0.2
298.15	1.20139	1.20579	1.20987
303.15	1.19856	1.20298	1.20706
308.15	1.19570	1.20015	1.20425
313.15	1.19283	1.19731	1.20147
318.15	1.18997	1.19446	1.19866
323.15	1.18709	1.19160	1.19584
328.15	1.18423	1.18874	1.19301
333.15	1.18136	1.18589	1.19019
338.15	1.17851	1.18304	1.18736
343.15	1.17565	1.18018	1.18453

Measurement are performed at atmospheric pressure.

Table 17. Density versus temperature data for DES (1:4, 1:4:0.1 and 1:4:0.2) over the temperature range (298.15-343.15) K

T/K	1 : 4	1 : 4 : 0.1	1 : 4 : 0.2
298.15	1.20945	1.21241	1.21644
303.15	1.20656	1.20956	1.21357
308.15	1.20364	1.20668	1.21074
313.15	1.20071	1.20379	1.20789
318.15	1.19776	1.20088	1.20502
323.15	1.19482	1.19797	1.20214
328.15	1.19187	1.19505	1.19926
333.15	1.18893	1.19214	1.19638
338.15	1.18597	1.18922	1.19350
343.15	1.18301	1.18630	1.19062

Measurement are performed at atmospheric pressure.

Table 18. Result of regression analysis of density versus temperature data according to equation for DES over the temperature range (298.15-343.15) K

DES / LTTM	m	c	r²
1 : 2	-0.0005564	1.3537245	0.9999974
1 : 2 : 0.1	-0.0005511	1.3592241	0.9999986
1 : 2 : 0.2	-0.0005494	1.3636345	0.9999966
1 : 3	-0.0005735	1.3727640	0.9999983
1 : 3 : 0.1	-0.0005697	1.3756763	0.9999947
1 : 3 : 0.2	-0.0005630	0.3777341	0.9999939
1 : 4	-0.0005873	1.3851820	0.9999920
1 : 4 : 0.1	-0.0005809	1.3856575	0.9999894
1 : 4 : 0.2	-0.0005738	1.3875469	0.9999934

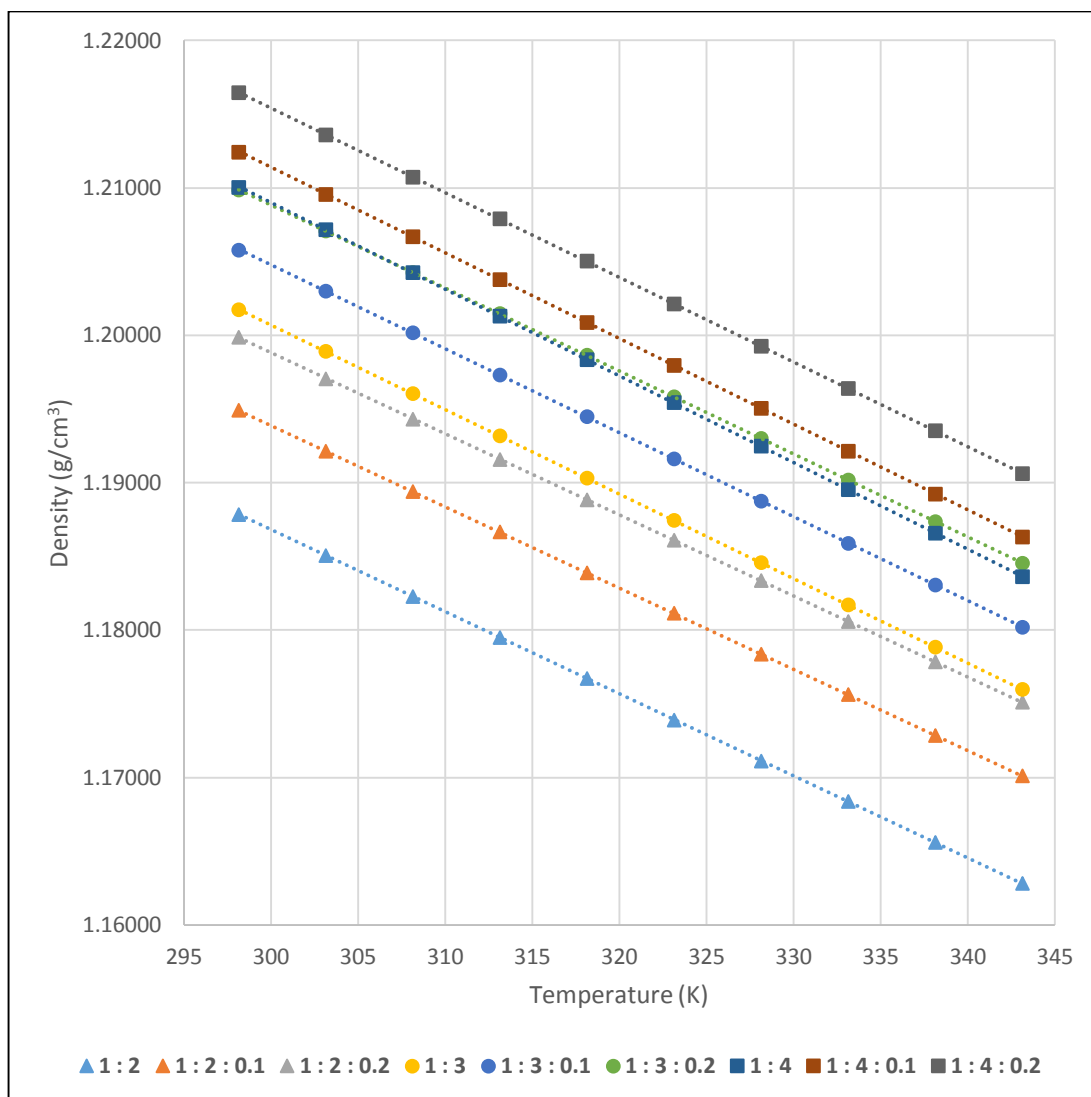


Figure 24. Density of DES against temperature range (298.15-343.15) K

4.4.2 Viscosity

Viscosity is a measure of resistance of fluid against shear stress and expression of strength of the molecular interactions within components of a fluid. It is a very significant parameter as it strongly influences the diffusion of dissolved particles in the solvent. The viscosities of DES has been measured as a function of temperature and are displayed in Figure 25 and Table 20 to 22. It can be noticed that increment of glycerol and arginine in the DES system will significantly increase the viscosity of DES, since adding more glycerol into the DES will produces composite viscosity closer to pure glycerol [30] which is 1412cP [54] at STP, whereas adding more arginine into the DES encourage a more efficient hydrogen bonding between components in DES [51]. The viscosity binary DES of 1 ChCl : 2 Glycerol is

compared with various literature review and the AAD% is found to range from 0.643% to 25.064% with an average of 9.649%. The high AAD% found in the experimental data is due to high uncertainties associated with falling ball viscosity measurement method, since the measurement can be done through different diameter of calibrated glass capillaries for the same range of viscosity.

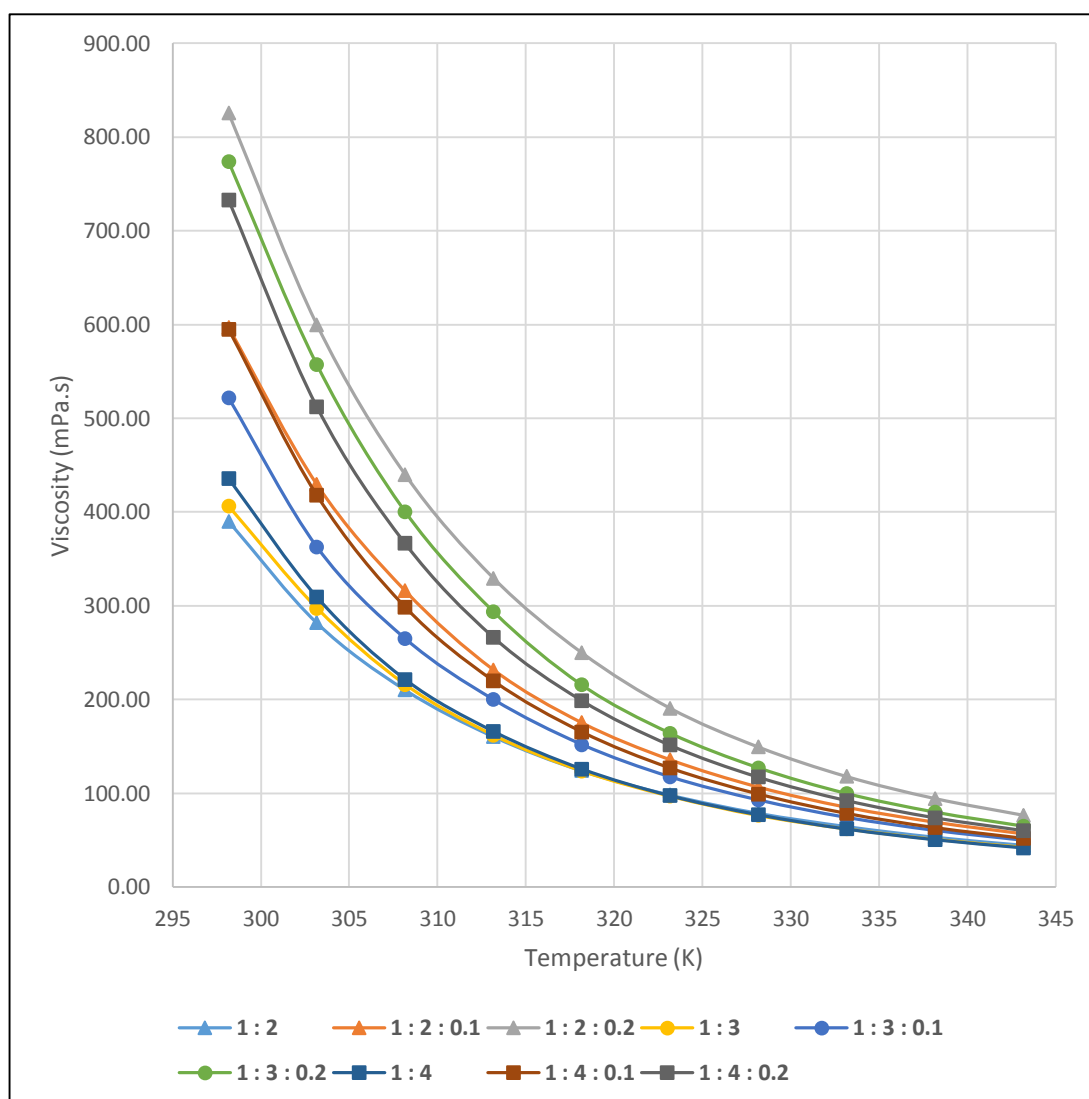


Figure 25. Viscosity of DES against temperature range (298.15-343.15) K

Table 19. Viscosity versus temperature data for DES (1:2, 1:2 (lit.), 1:2:0.1 and 1:2:0.2) over the temperature range (298.15-343.15) K

T/K	1 : 2	1 : 2 (lit.)	1 : 2 : 0.1	1 : 2 : 0.2
298.15	390.17	359 ^a	597.03	825.70

		376 ^b		
303.15	281.76	246.7928 ^c 376 ^d	429.53	600.00
308.15	210.24	259 ^d	316.04	440.00
313.15	160.45	133.3749 ^c 188 ^d	231.76	329.50
318.15	123.99	140 ^d	175.29	249.90
323.15	98.20	81.5895 ^c 104 ^d	135.82	190.70
328.15	78.73	82 ^d	106.63	149.30
333.15	64.58	53.8117 ^c 64 ^d	85.05	117.80
338.15	53.23	52 ^d	69.16	94.33
343.15	44.64	36.7409 ^c	56.76	76.53

Measurement are performed at atmospheric pressure. ^aRef. [49], ^bRef. [31], ^cRef [33], ^dRef [43]

Table 20. Viscosity versus temperature data for DES (1:3, 1:3:0.1 and 1:3:0.2) over the temperature range (298.15-343.15) K

T/K	1 : 3	1 : 3 (lit.)	1 : 3 : 0.1	1 : 3 : 0.2
298.15	406.08	450 ^a	521.80	773.80
303.15	297.43	320 ^a	362.80	557.30
308.15	215.92	229 ^a	264.90	400.40
313.15	161.85	169 ^a	199.90	293.80
318.15	123.71	126 ^a	151.90	215.60
323.15	96.74	95 ^a	117.40	164.10
328.15	76.18	73 ^a	92.69	127.20
333.15	61.85	58 ^a	74.06	99.74
338.15	50.76	-	60.15	79.91
343.15	42.34	-	49.68	64.94

Measurement are performed at atmospheric pressure. ^aRef [43]

Table 21. Viscosity versus temperature data for DES (1:4, 1:4:0.1 and 1:4:0.2) over the temperature range (298.15-343.15) K

T/K	1 : 4	1 : 4 (lit.)	1 : 4 : 0.1	1 : 4 : 0.2
298.15	435.60	503 ^a	595.10	733.10
303.15	309.20	350 ^a	418.10	512.50
308.15	221.40	246 ^a	298.80	366.60
313.15	166.00	178 ^a	220.00	266.50
318.15	125.95	132 ^a	165.60	199.00
323.15	97.37	98 ^a	127.00	151.40
328.15	77.10	86 ^a	99.23	117.30
333.15	61.81	57 ^a	78.53	92.33
338.15	50.47	-	63.36	73.99
343.15	41.77	-	51.96	60.32

Measurement are performed at atmospheric pressure. ^aRef [43]

Overall, viscosity decreased with increasing temperature (Figure 25) and at high temperature all binary DES tend to converged to one point which is around 43mPa.s while viscosity at high temperature of ternary DES with 0.1 and 0.2 molar ratio of arginine tend to converge towards 53mPa.s and 70mPa.s respectively. The dependence of viscosity towards temperature can be described through Vogel-Tamman-Fulcher (VTF) equation below:

$$\ln(\eta) = a + \frac{b}{T - c} \quad \text{Equation 9}$$

where η (mPa.s) is the dynamic viscosity, T is the temperature in Kelvin while a, b, and c are fitting parameters (Table 23). The fitting parameters are determined based on graph plotting of $\ln \eta$ versus $1/T$ as in Figure 26.

Table 22. Result of regression analysis of $\ln \eta$ versus $1/T$ according to equation for DES over the temperature range (298.15-343.15) K

DES / LTTM	a	b	c	r²
1 : 2	-1.6248756	854.3698963	185.6075460	0.9999913
1 : 2 : 0.1	-2.5842523	1131.2581214	172.2650319	0.9999296
1 : 2 : 0.2	-4.7629315	1968.5868578	126.6930620	0.9999773
1 : 3	-2.7139689	956.1136996	181.4340161	0.9999056

1 : 3 : 0.1	-2.1428772	974.4210759	182.0659508	0.9999473
1 : 3 : 0.2	-3.3894317	1366.8183080	162.2711349	0.9998501
1 : 4	-1.9669345	878.1435864	189.0288969	0.9999811
1 : 4 : 0.1	-2.4934613	1053.6117359	179.5629486	0.9999926
1 : 4 : 0.2	-2.7632310	1152.9119213	175.0464076	0.9999833

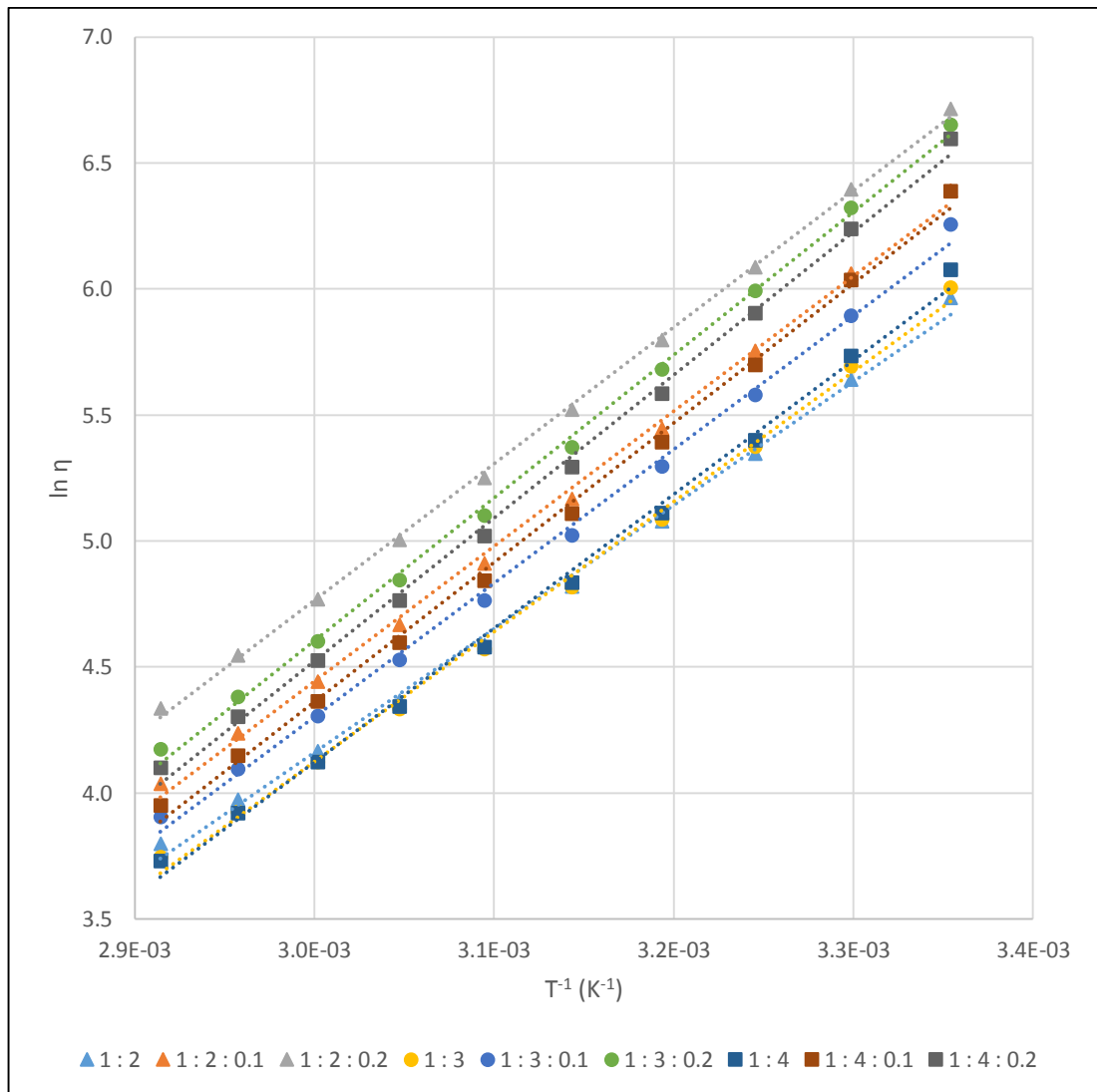


Figure 26. $\ln \eta$ against $1/T$ plot for all DES

4.4.3 Refractive Index

As part of physical properties measurement, refractive index of all DES is measured. Refractive index is the ratio of the velocity of light (sodium D line, 589nm wavelength [55]) in air to the velocity of light in the solvent. It is important as an

effort to determine the purity of solvent or concentration of components in a fluid. The refractive index of DES has been measured as a function of temperature and are displayed in Figure 27 and Table 24 to 26. It can be noticed that refractive index of DES reduces with increment of glycerol but increase with increment of arginine in the system. The refractive index of binary DES of 1 ChCl : 2 Glycerol is compared with various literature review and the AAD% is found to range from 0.125% to 0.129% with an average of 0.127%. Overall, refractive decreased with increasing temperature (figure 27). The data obtained in Table are then plotted into a graph to study the dependence of refractive index towards temperature, and fitting it through the equation 10.

$$\eta = mT + c \quad \text{Equation 10}$$

where η is refractive index of DES, T is temperature in Kelvin while m and c are the fitting parameters varied for different binary and ternary DES. Table shows the fitting parameters of density of each DES.

Table 23. Refractive index versus temperature data for DES (1:2, 1:2 (lit.), 1:2:0.1 and 1:2:0.2) over the temperature range (298.15-333.15) K

T/K	1 : 2	1 : 2 (lit.)	1 : 2 : 0.1	1 : 2 : 0.2
298.15	1.48489	1.48675 ^a	1.48939	1.49329
303.15	1.48372	1.48558 ^a	1.48825	1.49216
308.15	1.48256	1.48443 ^a	1.48709	1.49101
313.15	1.48137	1.48326 ^a	1.48593	1.48986
318.15	1.48021	1.48211 ^a	1.48476	1.48870
323.15	1.47905	1.48093 ^a	1.48361	1.48755
328.15	1.47787	1.47978 ^a	1.48244	1.48639
333.15	1.47670	1.47856 ^a	1.48127	1.48522

Measurement are performed at atmospheric pressure. ^aRef. [41]

Table 24. Refractive index versus temperature data for DES (1:3, 1:3:0.1 and 1:3:0.2) over the temperature range (298.15-333.15) K

T/K	1 : 3	1 : 3 : 0.1	1 : 3 : 0.2
298.15	1.48181	1.48405	1.48872

303.15	1.48066	1.48294	1.48756
308.15	1.47949	1.48177	1.48640
313.15	1.47830	1.48060	1.48522
318.15	1.47712	1.47943	1.48405
323.15	1.47594	1.47827	1.48288
328.15	1.47474	1.47708	1.48169
333.15	1.47354	1.47589	1.48050

Measurement are performed at atmospheric pressure.

Table 25. Refractive index versus temperature data for DES (1:4, 1:4:0.1 and 1:4:0.2) over the temperature range (298.15-333.15) K

T/K	1 : 4	1 : 4 : 0.1	1 : 4 : 0.2
298.15	1.47977	1.48145	1.48620
303.15	1.47861	1.48030	1.48503
308.15	1.47743	1.47911	1.48383
313.15	1.47622	1.47793	1.48264
318.15	1.47503	1.47674	1.48145
323.15	1.47384	1.47555	1.48026
328.15	1.47262	1.47435	1.47905
333.15	1.47142	1.47313	1.47785

Measurement are performed at atmospheric pressure.

Table 26. Result of regression analysis of refractive index versus temperature data according to equation for DES over the temperature range (298.15-333.15) K

DES / LTTM	m	c	r²
1 : 2	-0.0002341	1.5546901	0.9999973
1 : 2 : 0.1	-0.0002323	1.5586643	0.9999890
1 : 2 : 0.2	-0.0002309	1.5621526	0.9999844
1 : 3	-0.0002366	1.5523696	0.9999659
1 : 3 : 0.1	-0.0002335	1.5537222	0.9999491
1 : 3 : 0.2	-0.0002348	1.5587349	0.9999845
1 : 4	-0.0002389	1.5510178	0.9999619

1 : 4 : 0.1	-0.0002378	1.5523687	0.9999599
1 : 4 : 0.2	-0.0002388	1.5574236	0.9999886

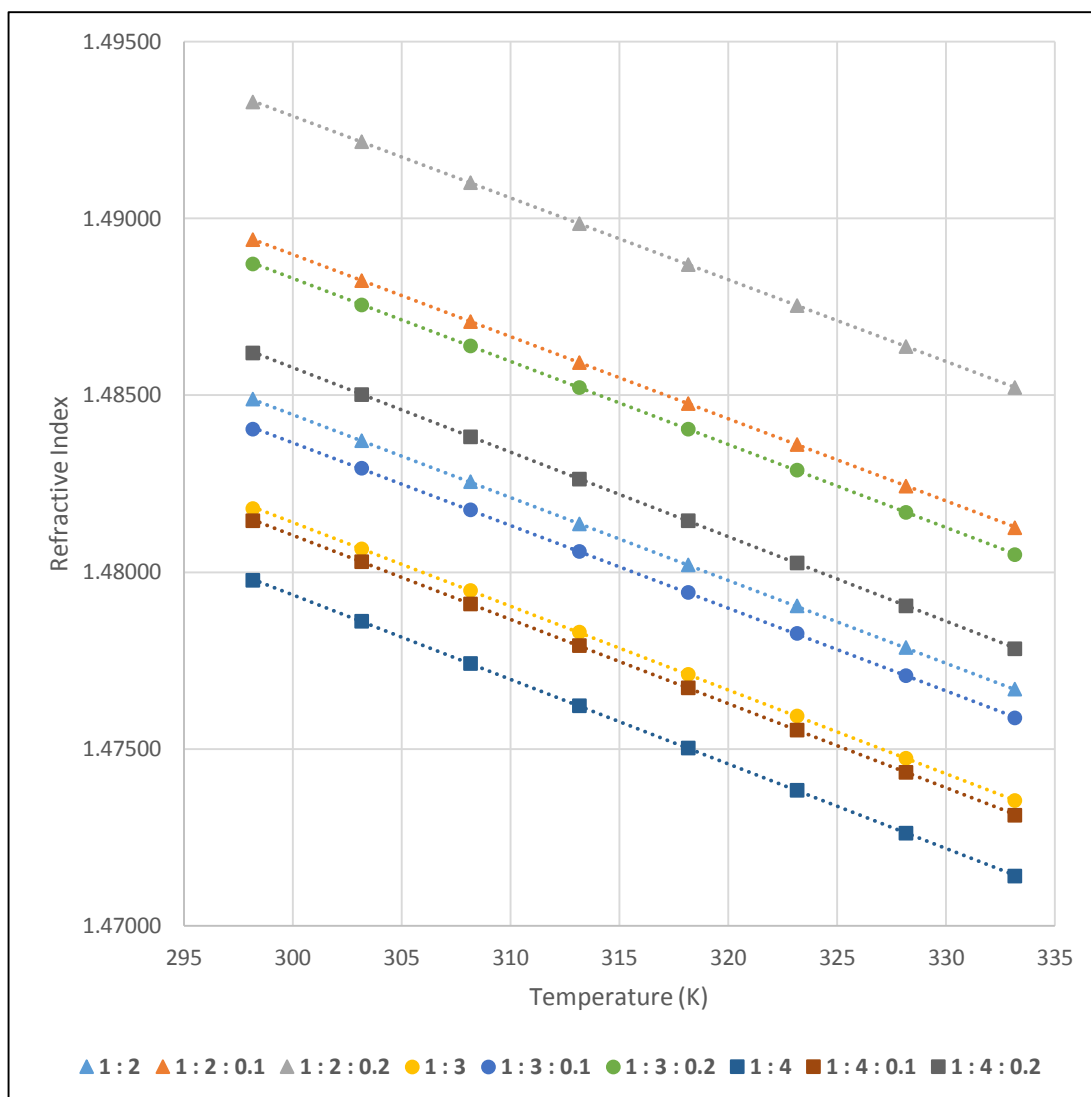


Figure 27. Refractive index of DES against temperature range (298.15-333.15) K

CHAPTER 5

CONCLUSION

A variety ratio of DES are synthesized by mixing glyceline of different HBD ratio with L-Arg. Decomposition temperature and melting point are measured and the physical properties including density, viscosity and refractive index of DES and LTTM are studied at ambient pressure and different temperatures from (298.15 up to 333.15) K. The result show that the mole ratio of HBD of glyceline and mole ratio of L-Arg have strong effect on the physical properties. Density, viscosity and refractive index of DES and LTTM decrease with an increase of temperature and an increase of L-Arg content. Unlike density and viscosity, refractive index, however decrease with an increase with of HBD content. An empirical linear equation could be used to correlate density, and refractive index as a function of temperature while VTF equation is used as fittings to the viscosity to correlate the dependence of viscosity towards temperature.

REFERENCES

- [1] G. Li, D. Deng, Y. Chen, H. Shan, and N. Ai, "Solubilities and thermodynamic properties of CO₂ in choline-chloride based deep eutectic solvents," *The Journal of Chemical Thermodynamics*, vol. 75, pp. 58-62, 8// 2014.
- [2] J. Li, Y. Ye, L. Chen, and Z. Qi, "Solubilities of CO₂ in Poly(ethylene glycols) from (303.15 to 333.15) K," *Journal of Chemical & Engineering Data*, vol. 57, pp. 610-616, 2012/02/09 2011.
- [3] A. Yamasaki, "An Overview of CO₂ Mitigation Options for Global Warming—Emphasizing CO₂ Sequestration Options," *JOURNAL OF CHEMICAL ENGINEERING OF JAPAN*, vol. 36, pp. 361-375, 2003.
- [4] IEA, "Key World Energy Statistics," 2014.
- [5] co2now.org, "Earth's CO₂," 2014.
- [6] J. Amos, "Deep ice tells long climate story," 2006.
- [7] IChemE, "More urgency needed for coal power plant re-design," 2014.
- [8] S. A. Ebenezer, "REMOVAL OF CARBON DIOXIDE FROM NATURAL GAS FOR LNG PRODUCTION," 2005.
- [9] N. Rodríguez, S. Mussati, and N. Scenna, "Optimization of post-combustion CO₂ process using DEA–MDEA mixtures," *Chemical Engineering Research and Design*, vol. 89, pp. 1763-1773, 9// 2011.
- [10] N. Dave, T. Do, G. Puxty, R. Rowland, P. H. M. Feron, and M. I. Attalla, "CO₂ capture by aqueous amines and aqueous ammonia—A Comparison," *Energy Procedia*, vol. 1, pp. 949-954, 2// 2009.
- [11] M. K. Hanne, Rochelle, G.T., "Effects of the temperature bulge in CO₂ absorption from flue gas by aqueous monoethanolamine," *Ind. Eng. Chem. Res.*, p. 9, 2008.

- [12] B. R. Anand, Rubin, E.S., Keith, D.W., Morgan, M.G., "Evaluation of potential cost reductions from improved amine-based CO₂ capture systems," *Energy Policy*, vol. 34, p. 8, 2006.
- [13] Q. Ye, Y. Zhang, M. Li, and Y. Shi, "Adsorption of low concentration CO₂ by modified carbon nanotubes under ambient temperature," *Wuli Huaxue Xuebao/Acta Physico - Chimica Sinica*, vol. 28, pp. 1223-1229, 2012.
- [14] G. T. Rochelle, "Amine Scrubbing for CO₂ Capture," *Science*, vol. 325, pp. 1652-1654, September 25, 2009 2009.
- [15] M. Hasib-ur-Rahman, M. Siaj, and F. Larachi, "Ionic liquids for CO₂ capture—Development and progress," *Chemical Engineering and Processing: Process Intensification*, vol. 49, pp. 313-322, 4// 2010.
- [16] C. Pretti, C. Chiappe, D. Pieraccini, M. Gregori, F. Abramo, G. Monni, *et al.*, "Acute toxicity of ionic liquids to the zebrafish (*Danio rerio*)," *Green Chemistry*, vol. 8, pp. 238-240, 2006.
- [17] J. Kumelan, Á. Pérez-Salado Kamps, D. Tuma, and G. Maurer, "Solubility of CO₂ in the ionic liquid [hmim][Tf₂N]," *The Journal of Chemical Thermodynamics*, vol. 38, pp. 1396-1401, 11// 2006.
- [18] R. J. Bernot, E. E. Kennedy, and G. A. Lamberti, "Effects of ionic liquids on the survival, movement, and feeding behavior of the freshwater snail, *Physa acuta*," *Environmental Toxicology and Chemistry*, vol. 24, pp. 1759-1765, 2005.
- [19] R. E. Baltus, B. H. Culbertson, S. Dai, H. Luo, and D. W. DePaoli, "Low-Pressure Solubility of Carbon Dioxide in Room-Temperature Ionic Liquids Measured with a Quartz Crystal Microbalance," *The Journal of Physical Chemistry B*, vol. 108, pp. 721-727, 2004/01/01 2003.
- [20] L. A. Blanchard, Z. Gu, and J. F. Brennecke, "High-Pressure Phase Behavior of Ionic Liquid/CO₂ Systems," *The Journal of Physical Chemistry B*, vol. 105, pp. 2437-2444, 2001/03/01 2001.

- [21] L. A. Blanchard, D. Hancu, E. J. Beckman, and J. F. Brennecke, "Green processing using ionic liquids and CO₂," *Nature*, vol. 399, pp. 28-29, 05/06/print 1999.
- [22] P. Husson-Borg, V. Majer, and M. F. Costa Gomes, "Solubilities of Oxygen and Carbon Dioxide in Butyl Methyl Imidazolium Tetrafluoroborate as a Function of Temperature and at Pressures Close to Atmospheric Pressure†," *Journal of Chemical & Engineering Data*, vol. 48, pp. 480-485, 2003/05/01 2003.
- [23] C. Ye and J. n. M. Shreeve, "Rapid and Accurate Estimation of Densities of Room-Temperature Ionic Liquids and Salts," *The Journal of Physical Chemistry A*, vol. 111, pp. 1456-1461, 2007/03/01 2007.
- [24] D. J. Couling, R. J. Bernot, K. M. Docherty, J. K. Dixon, and E. J. Maginn, "Assessing the factors responsible for ionic liquid toxicity to aquatic organisms via quantitative structure-property relationship modeling," *Green Chemistry*, vol. 8, pp. 82-90, 2006.
- [25] A. Latała, P. Stepnowski, M. Nędzi, and W. Mroziak, "Marine toxicity assessment of imidazolium ionic liquids: Acute effects on the Baltic algae *Oocystis submarina* and *Cyclotella meneghiniana*," *Aquatic Toxicology*, vol. 73, pp. 91-98, 6/1/ 2005.
- [26] A. P. Abbott, D. Boothby, G. Capper, D. L. Davies, and R. K. Rasheed, "Deep Eutectic Solvents Formed between Choline Chloride and Carboxylic Acids: Versatile Alternatives to Ionic Liquids," *Journal of the American Chemical Society*, vol. 126, pp. 9142-9147, 2004/07/01 2004.
- [27] R. B. Leron and M.-H. Li, "High-pressure density measurements for choline chloride: Urea deep eutectic solvent and its aqueous mixtures at T= (298.15 to 323.15) K and up to 50 MPa," *The Journal of Chemical Thermodynamics*, vol. 54, pp. 293-301, 11// 2012.
- [28] "Biocatalysis in Sustainable Solvents Made from Chicken Feed and Fertilizer," *Chem. Commun.*, p. 3, 2008.

- [29] M. Francisco, A. van den Bruinhorst, L. F. Zubeir, C. J. Peters, and M. C. Kroon, "A new low transition temperature mixture (LTTM) formed by choline chloride+lactic acid: Characterization as solvent for CO₂ capture," *Fluid Phase Equilibria*, vol. 340, pp. 77-84, 2/25/ 2013.
- [30] F. M. J. Naser, B. Jibril, S. Al-Hatmi, and Z. Gano, "Potassium Carbonate as a Salt for Deep Eutectic Solvents," *International Journal of Chemical Engineering and Applications*, vol. 4, pp. 114-118, 2013.
- [31] E. L. Smith, A. P. Abbott, and K. S. Ryder, "Deep Eutectic Solvents (DESs) and Their Applications," *Chem Rev*, Oct 10 2014.
- [32] Y.-T. Liu, Y.-A. Chen, and Y.-J. Xing, "Synthesis and characterization of novel ternary deep eutectic solvents," *Chinese Chemical Letters*, vol. 25, pp. 104-106, 1// 2014.
- [33] A. Yadav, S. Trivedi, R. Rai, and S. Pandey, "Densities and dynamic viscosities of (choline chloride+glycerol) deep eutectic solvent and its aqueous mixtures in the temperature range (283.15–363.15)K," *Fluid Phase Equilibria*, vol. 367, pp. 135-142, 2014.
- [34] H. J. Wang, Y.; Wang, X.; Yao, Y.; Jia, Y, *J. Mol. Liqu*, vol. 163, 2011.
- [35] P. J. Atkins. P., "Atkins' Physical Chemistry 8th edition."
- [36] "Plastics – Differential scanning calorimetry (DSC) – Part 2: Determination of glass transition temperature," 1999.
- [37] P. G. S. Debenedetti, "Supercooled liquids and the glass transition," *Nature*, vol. 410, pp. 259-267, 2001.
- [38] J. Zarzycki, "Glasses and the Vitreous State," *Cambridge University Press*, 1991.
- [39] "glass-transition temperature," *IUPAC Compendium of Chemical Terminology*, vol. 66, 1984.
- [40] R. B. Leron, D. S. H. Wong, and M.-H. Li, "Densities of a deep eutectic solvent based on choline chloride and glycerol and its aqueous mixtures at elevated pressures," *Fluid Phase Equilibria*, vol. 335, pp. 32-38, 12/15/ 2012.

- [41] R. B. Leron, A. N. Soriano, and M.-H. Li, "Densities and refractive indices of the deep eutectic solvents (choline chloride+ethylene glycol or glycerol) and their aqueous mixtures at the temperature ranging from 298.15 to 333.15K," *Journal of the Taiwan Institute of Chemical Engineers*, vol. 43, pp. 551-557, 2012.
- [42] L. L. Sze, S. Pandey, S. Ravula, S. Pandey, H. Zhao, G. A. Baker, *et al.*, "Ternary Deep Eutectic Solvents Tasked for Carbon Dioxide Capture," *Acs Sustainable Chemistry & Engineering*, vol. 2, pp. 2117-2123, Sep 2014.
- [43] a. R. C. H. Andrew P. Abbott, a Karl S. Ryder, a Carmine D'Agostino, b Lynn F. Gladdenb and Mick D. Mantleb, "Glycerol eutectics as sustainable solvent systems," *Green Chemistry*, vol. 13, pp. 82-90, 2011.
- [44] PunChem, "Open Chemistry Database," 2014.
- [45] R. B. Leron and M.-H. Li, "Solubility of carbon dioxide in a eutectic mixture of choline chloride and glycerol at moderate pressures," *The Journal of Chemical Thermodynamics*, vol. 57, pp. 131-136, 2// 2013.
- [46] C.-M. Lin, R. B. Leron, A. R. Caparanga, and M.-H. Li, "Henry's constant of carbon dioxide-aqueous deep eutectic solvent (choline chloride/ethylene glycol, choline chloride/glycerol, choline chloride/malonic acid) systems," *The Journal of Chemical Thermodynamics*, vol. 68, pp. 216-220, 1// 2014.
- [47] MayoClinic, "Arginine," <http://www.mayoclinic.org/drugs-supplements/arginine/background/hrb-20058733>, 2015.
- [48] D. Cojocari, "CRC Handbook of Chemistry," 2010.
- [49] Q. Zhang, K. De Oliveira Vigier, S. Royer, and F. Jerome, "Deep eutectic solvents: syntheses, properties and applications," *Chemical Society Reviews*, vol. 41, pp. 7108-7146, 2012.
- [50] D. Choudhury, R. C. Borah, R. L. Goswamee, H. P. Sharmah, and P. G. Rao, "Non-isothermal thermogravimetric pyrolysis kinetics of waste petroleum refinery sludge by isoconversional approach," *Journal of Thermal Analysis and Calorimetry*, vol. 89, pp. 965-970, 2007/09/01 2007.

- [51] L. F. Zubeir, M. H. M. Lacroix, and M. C. Kroon, "Low Transition Temperature Mixtures as Innovative and Sustainable CO₂ Capture Solvents," *The Journal of Physical Chemistry B*, vol. 118, pp. 14429-14441, 2014/12/11 2014.
- [52] Q. Abbas and L. Binder, "Synthesis and Characterization of Choline Chloride Based Binary Mixtures," *ECS Transactions*, vol. 33, pp. 49-59, October 1, 2010 2010.
- [53] K. Shahbaz, S. Baroutian, F. S. Mjalli, M. A. Hashim, and I. M. AlNashef, "Densities of ammonium and phosphonium based deep eutectic solvents: Prediction using artificial intelligence and group contribution techniques," *Thermochimica Acta*, vol. 527, pp. 59-66, 1/10/ 2012.
- [54] J. B. Segur and H. E. Oberstar, "Viscosity of Glycerol and Its Aqueous Solutions," *Industrial & Engineering Chemistry*, vol. 43, pp. 2117-2120, 1951/09/01 1951.
- [55] R. Miles, X. C. Zhang, H. Eisele, and A. Krotkus, *Terahertz Frequency Detection and Identification of Materials and Objects*: Springer Netherlands, 2007.

APPENDICES

Appendix 1 Thermal Curve and DSC Curve for All Solvent

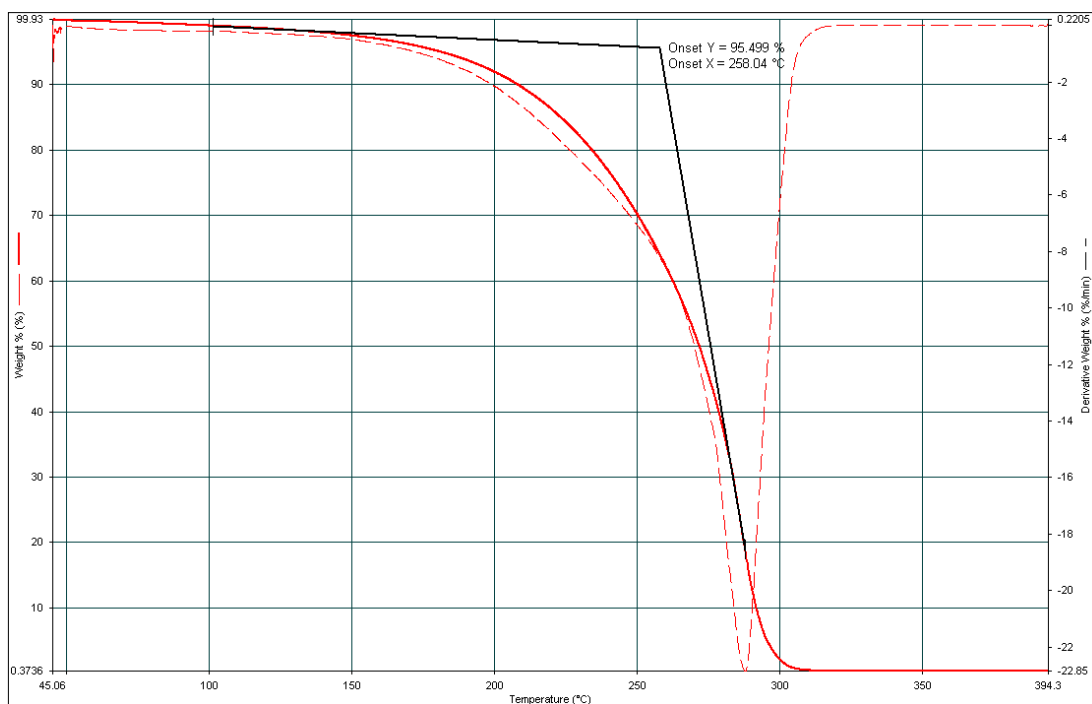


Figure 28. Thermal curve for DES/LTTM 1:2

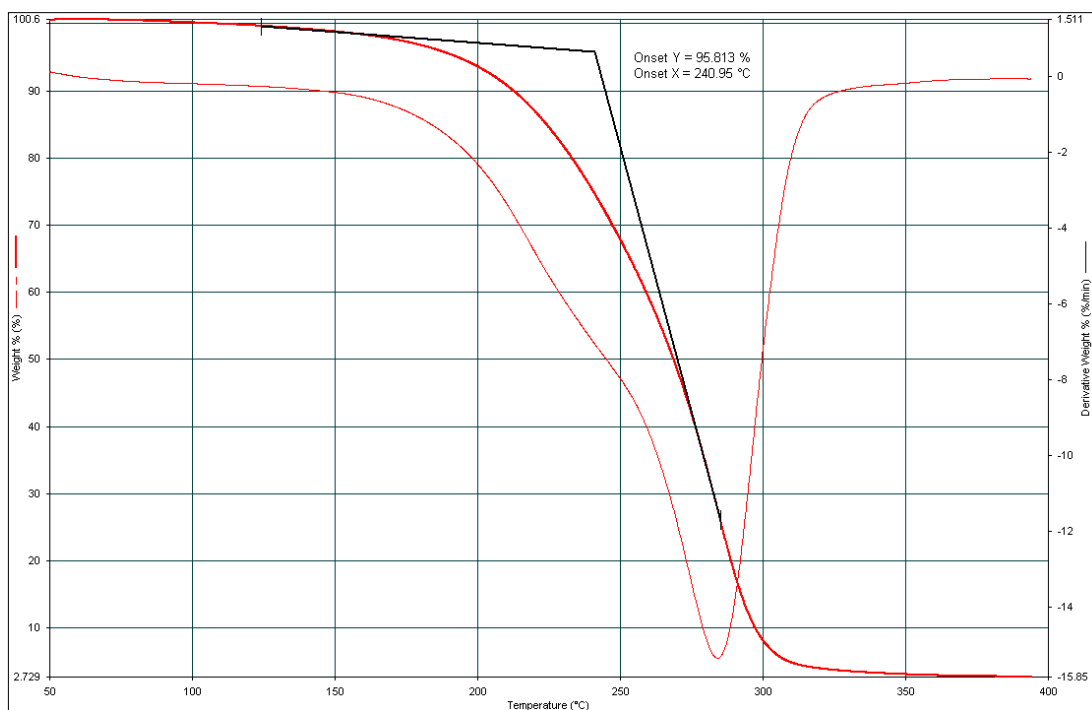


Figure 29. Thermal curve for DES/LTTM 1:2:0.1

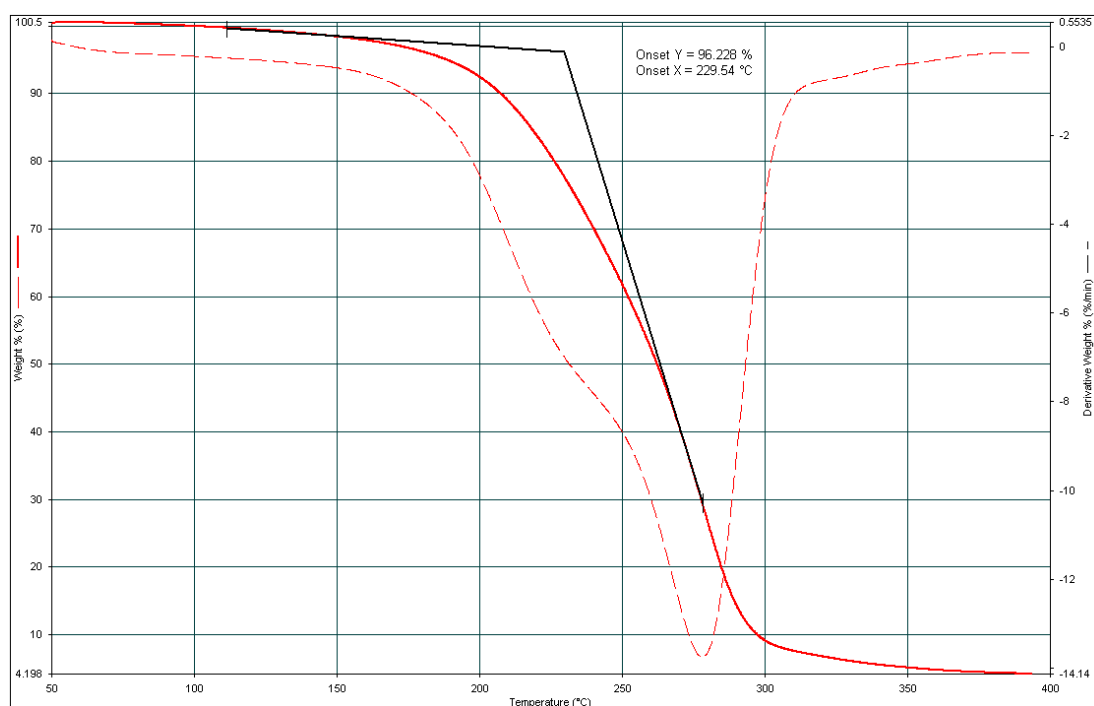


Figure 30. Thermal curve for DES/LTTM 1:2:0.2

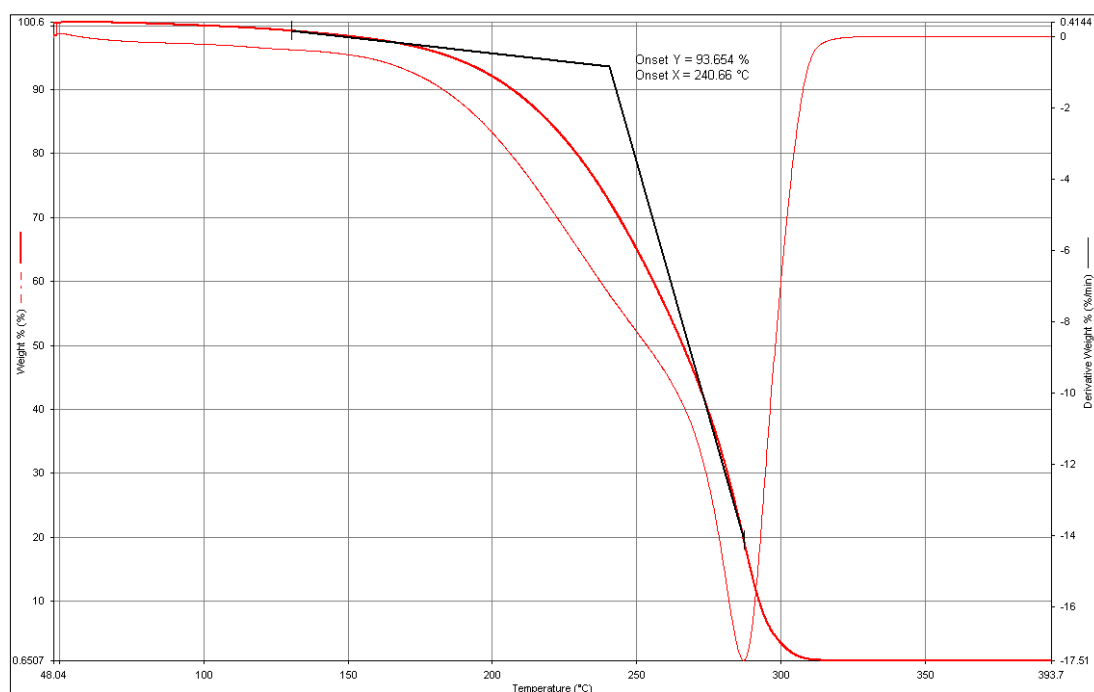


Figure 31. Thermal curve for DES/LTTM 1:3

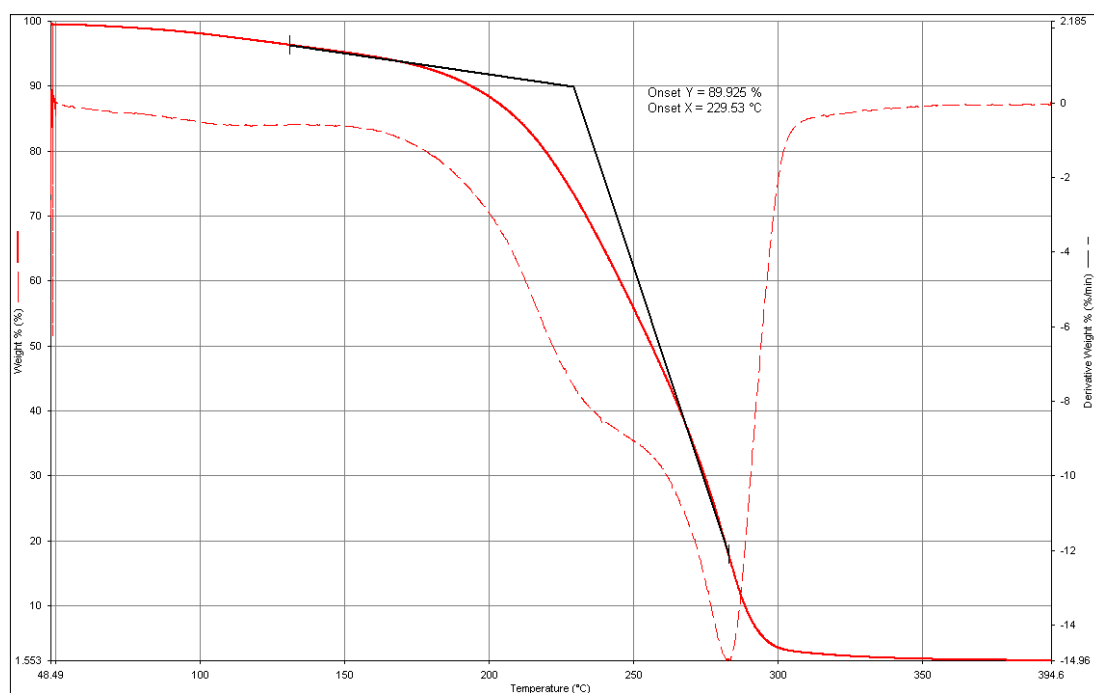


Figure 32. Thermal curve for DES/LTTM 1:3:0.1

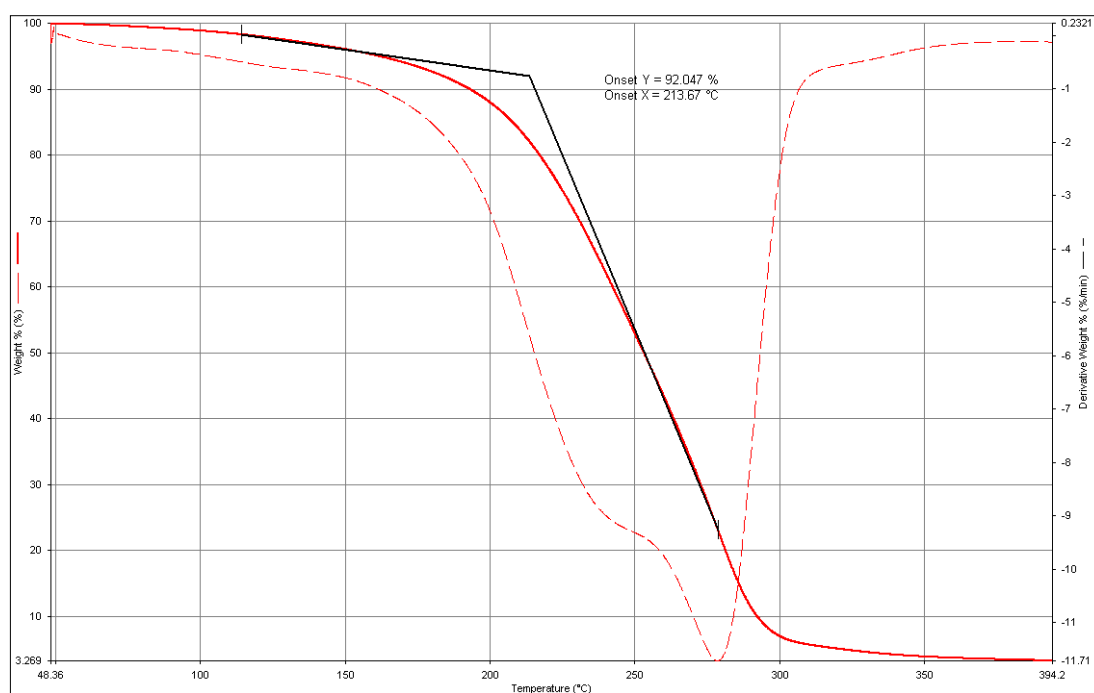


Figure 33. Thermal curve for DES/LTTM 1:3:0.2

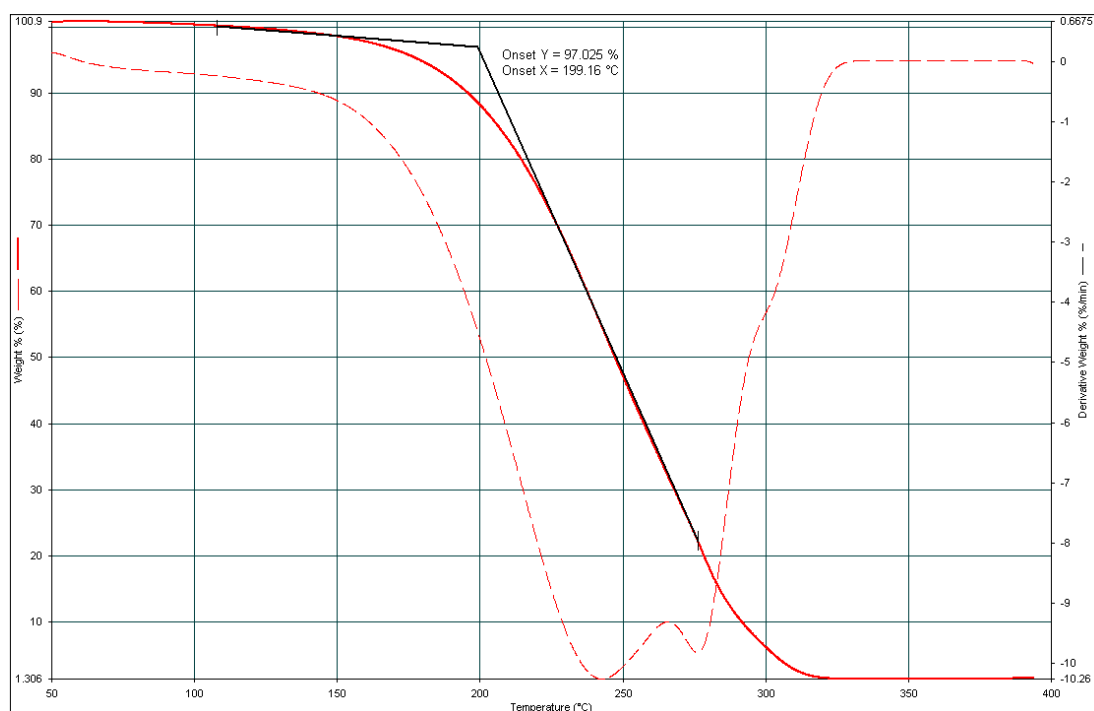


Figure 34. Thermal curve for DES/LTTM 1:4

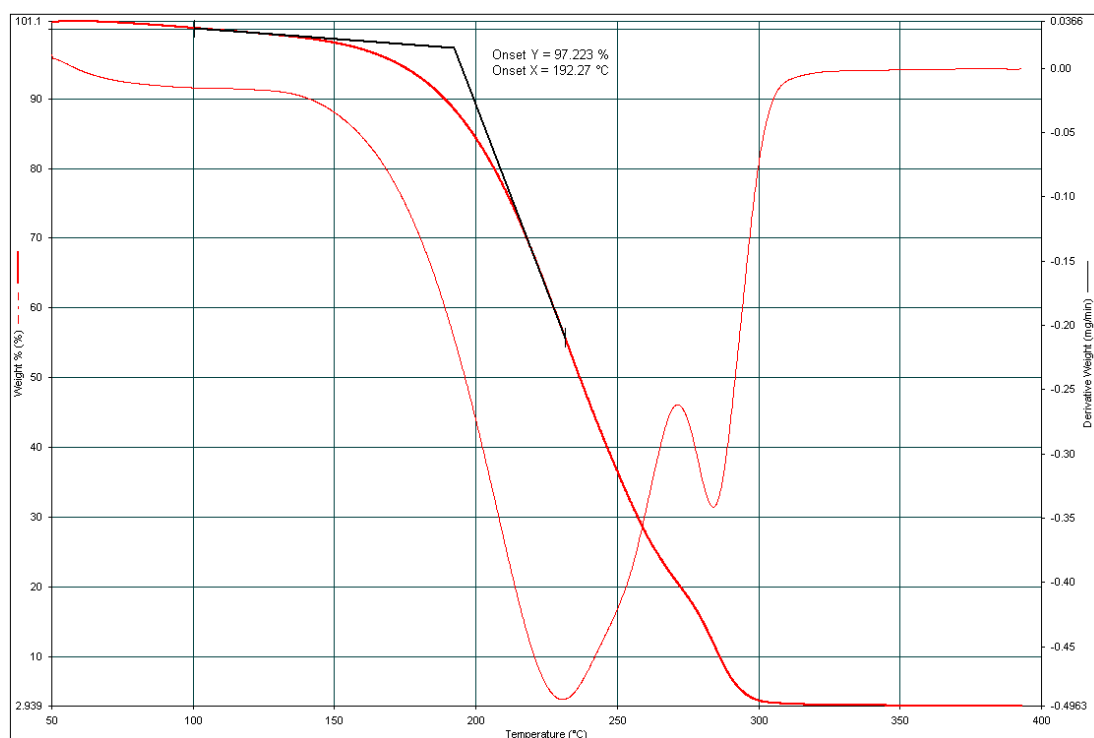


Figure 35. Thermal curve for DES/LTTM 1:4:0.1

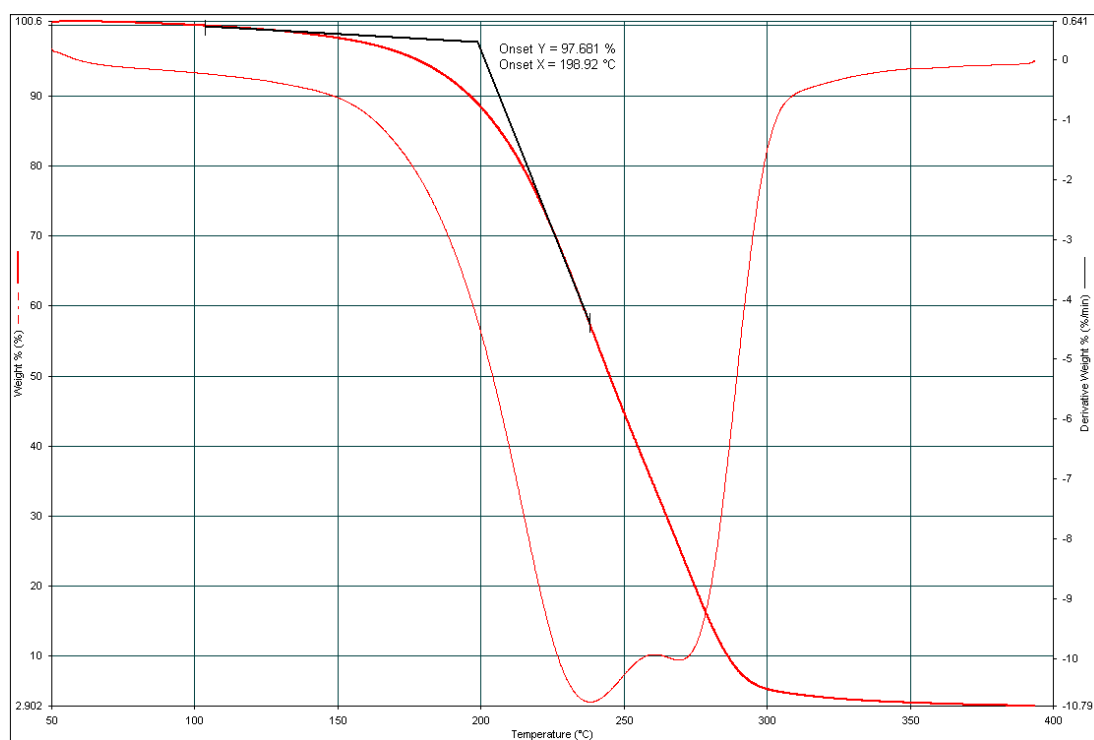


Figure 36. Thermal curve for DES/LTTM 1:4:0.2



Figure 37. DSC curve for DES/LTTM 1:2, 1:2:0.1 and 1:2:0.2

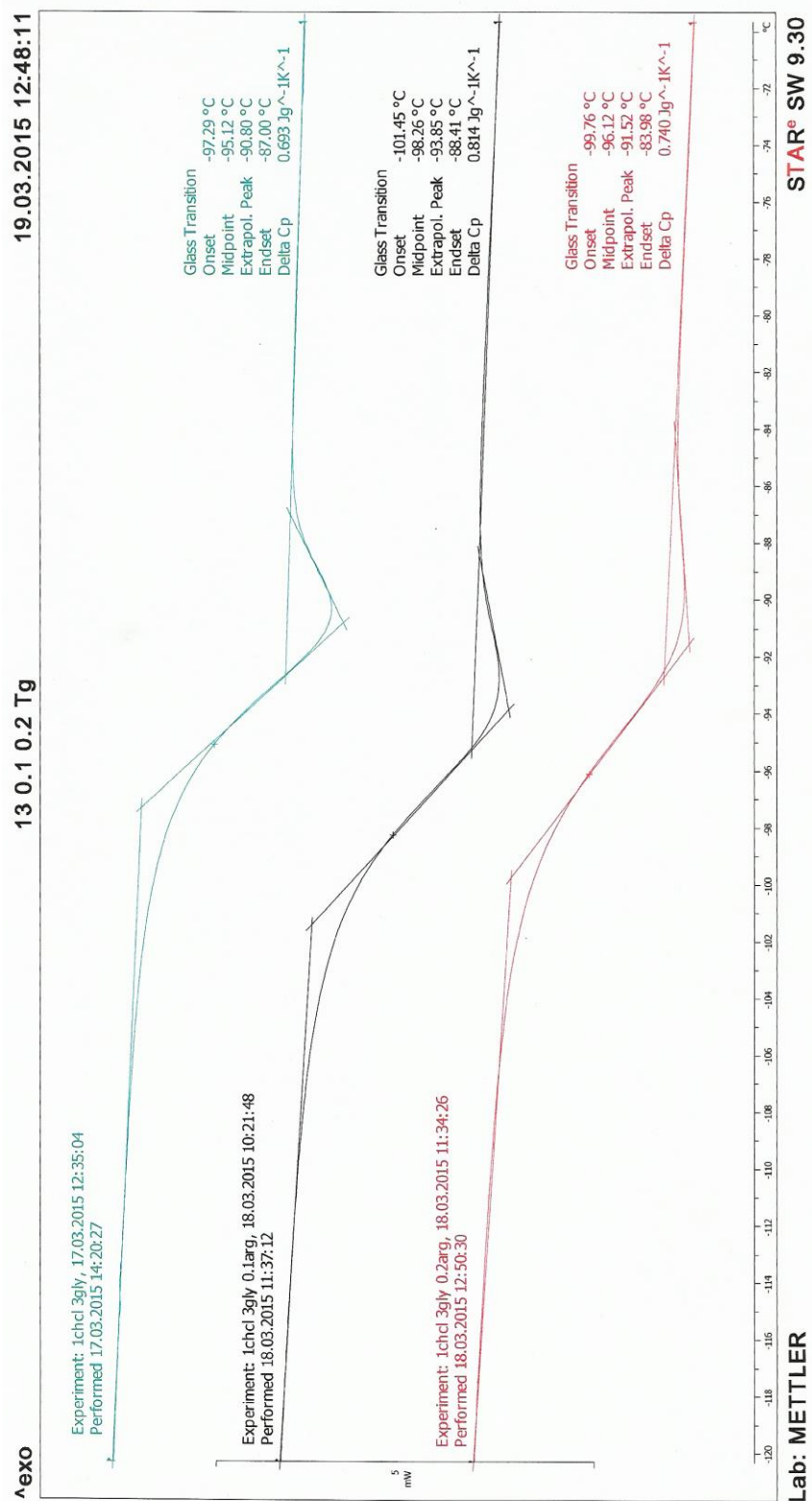


Figure 38. DSC curve for DES/LTTM 1:3, 1:3:0.1 and 1:3:0.2

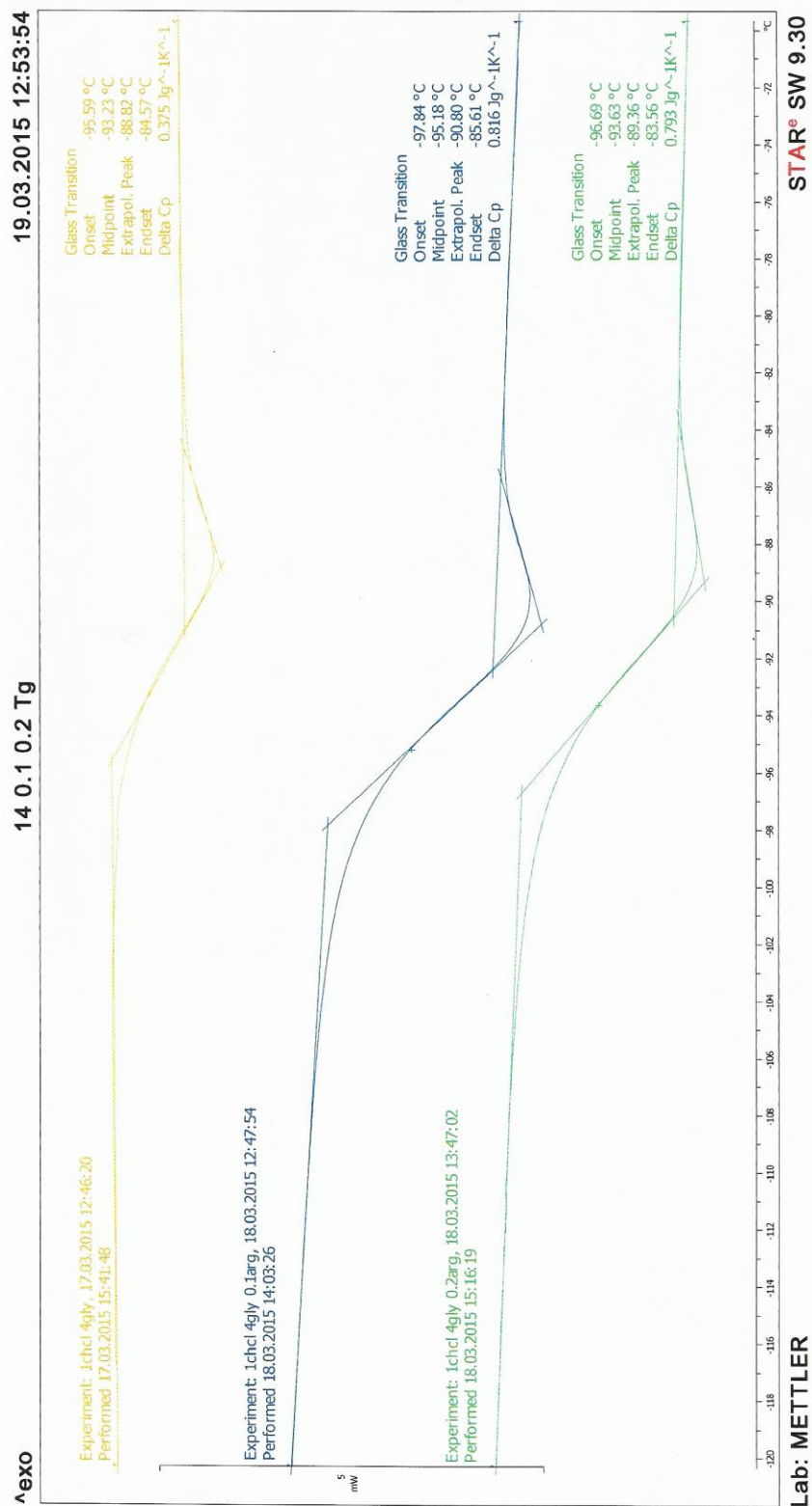


Figure 39. DSC curve for DES/LTTM 1:4, 1:4:0.1 and 1:4:0.2

Appendix 2 Raw Data Density, Viscosity and Refractive Index for All Solvent

Table 27. Raw Data Density

T/K	1 : 2			1 : 2 : 0.1			1 : 2 : 0.2		
298.15	1.18823	1.18782	1.18749	1.19442	1.19467	1.19559	1.19999	1.19993	1.19962
303.15	1.18546	1.18505	1.18471	1.19169	1.19192	1.19285	1.19718	1.19713	1.19683
308.15	1.18267	1.18226	1.18192	1.18895	1.18917	1.19011	1.19445	1.19439	1.19408
313.15	1.17986	1.17947	1.17913	1.18620	1.18641	1.18735	1.19173	1.19167	1.19134
318.15	1.17707	1.17668	1.17634	1.18344	1.18365	1.18460	1.18899	1.18894	1.18860
323.15	1.17429	1.17389	1.17356	1.18067	1.18088	1.18184	1.18625	1.18620	1.18584
328.15	1.17151	1.17111	1.17078	1.17791	1.17811	1.17908	1.18350	1.18345	1.18308
333.15	1.16874	1.16834	1.16801	1.17516	1.17534	1.17633	1.18075	1.18070	1.18031
338.15	1.16597	1.16557	1.16524	1.17242	1.17258	1.17358	1.17800	1.17797	1.17755
343.15	1.16321	1.16279	1.16247	1.16969	1.16983	1.17083	1.17526	1.17523	1.17479

Table 28. Raw Data Viscosity

T/K	1 : 2			1 : 2 : 0.1			1 : 2 : 0.2		
298.15	390.17	392.12	388.22	597.03	600.02	594.04	825.70	829.83	821.57
303.15	281.76	283.17	280.35	429.53	431.68	427.38	600.00	603.00	597.00
308.15	210.24	211.29	209.19	316.04	317.62	314.46	440.00	442.20	437.80
313.15	160.45	161.25	159.65	231.76	232.92	230.60	329.50	331.15	327.85
318.15	123.99	124.61	123.37	175.29	176.17	174.41	249.90	251.15	248.65
323.15	98.20	98.69	97.71	135.82	136.50	135.14	190.70	191.65	189.75
328.15	78.73	79.13	78.34	106.63	107.16	106.10	149.30	150.05	148.55
333.15	64.58	64.90	64.26	85.05	85.48	84.63	117.80	118.39	117.21
338.15	53.23	53.49	52.96	69.16	69.50	68.81	94.33	94.80	93.86
343.15	44.64	44.86	44.42	56.76	57.04	56.47	76.53	76.91	76.15

Table 29. Raw Data Refractive Index

T/K	1 : 2			1 : 2 : 0.1			1 : 2 : 0.2		
298.15	1.48494	1.48495	1.48479	1.48940	1.48936	1.48942	1.49334	1.49338	1.49316
303.15	1.48379	1.48376	1.48361	1.48826	1.48823	1.48826	1.49219	1.49223	1.49207
308.15	1.48263	1.48260	1.48244	1.48711	1.48707	1.48710	1.49104	1.49106	1.49094
313.15	1.48144	1.48142	1.48126	1.48595	1.48591	1.48593	1.48989	1.48990	1.48978
318.15	1.48028	1.48025	1.48009	1.48479	1.48474	1.48476	1.48873	1.48875	1.48863
323.15	1.47912	1.47909	1.47893	1.48364	1.48359	1.48361	1.48757	1.48759	1.48748
328.15	1.47795	1.47792	1.47774	1.48246	1.48242	1.48243	1.48641	1.48642	1.48633
333.15	1.47679	1.47674	1.47656	1.48130	1.48125	1.48125	1.48524	1.48524	1.48517

Table 30. Raw Data Density

T/K	1 : 3			1 : 3 : 0.1			1 : 3 : 0.2		
298.15	1.20176	1.20102	1.20246	1.20578	1.20626	1.20533	1.20972	1.21025	1.20963
303.15	1.19893	1.19818	1.19962	1.20298	1.20344	1.20251	1.20690	1.20744	1.20683
308.15	1.19607	1.19532	1.19676	1.20016	1.20062	1.19968	1.20410	1.20460	1.20405
313.15	1.19321	1.19245	1.19388	1.19732	1.19777	1.19684	1.20130	1.20186	1.20126
318.15	1.19034	1.18959	1.19101	1.19447	1.19492	1.19398	1.19847	1.19905	1.19846
323.15	1.18748	1.18670	1.18813	1.19162	1.19206	1.19112	1.19564	1.19623	1.19564
328.15	1.18461	1.18384	1.18526	1.18877	1.18921	1.18825	1.19280	1.19340	1.19283
333.15	1.18175	1.18097	1.18237	1.18593	1.18635	1.18539	1.18996	1.19058	1.19002
338.15	1.17890	1.17811	1.17948	1.18308	1.18350	1.18253	1.18713	1.18775	1.18720
343.15	1.17606	1.17524	1.17657	1.18022	1.18064	1.17967	1.18429	1.18493	1.18437

Table 31. Raw Data Viscosity

T/K	1 : 3			1 : 3 : 0.1			1 : 3 : 0.2		
298.15	406.08	405.27	406.89	521.80	520.76	522.84	773.80	772.25	775.35
303.15	297.43	296.84	298.02	362.80	362.07	363.53	557.30	556.19	558.41
308.15	215.92	215.49	216.35	264.90	264.37	265.43	400.40	399.60	401.20
313.15	161.85	161.53	162.17	199.90	199.50	200.30	293.80	293.21	294.39
318.15	123.71	123.46	123.96	151.90	151.60	152.20	215.60	215.17	216.03
323.15	96.74	96.55	96.94	117.40	117.17	117.63	164.10	163.77	164.43
328.15	76.18	76.02	76.33	92.69	92.50	92.88	127.20	126.95	127.45
333.15	61.85	61.73	61.98	74.06	73.91	74.21	99.74	99.54	99.94
338.15	50.76	50.65	50.86	60.15	60.03	60.27	79.91	79.75	80.07
343.15	42.34	42.25	42.42	49.68	49.58	49.78	64.94	64.81	65.07

Table 32. Raw Data Refractive Index

T/K	1 : 3			1 : 3 : 0.1			1 : 3 : 0.2		
298.15	1.48172	1.48186	1.48185	1.48406	1.48402	1.48408	1.48875	1.48869	1.48872
303.15	1.48060	1.48071	1.48068	1.48294	1.48292	1.48295	1.48758	1.48753	1.48757
308.15	1.47945	1.47952	1.47951	1.48176	1.48176	1.48178	1.48641	1.48638	1.48640
313.15	1.47827	1.47832	1.47832	1.48059	1.48059	1.48061	1.48523	1.48520	1.48522
318.15	1.47710	1.47713	1.47713	1.47943	1.47943	1.47944	1.48406	1.48403	1.48405
323.15	1.47592	1.47594	1.47595	1.47826	1.47827	1.47827	1.48289	1.48286	1.48289
328.15	1.47473	1.47474	1.47474	1.47708	1.47708	1.47708	1.48170	1.48167	1.48170
333.15	1.47354	1.47354	1.47355	1.47589	1.47589	1.47589	1.48051	1.48049	1.48050

Table 33. Raw Data Density

T/K	1 : 4			1 : 4 : 0.1			1 : 4 : 0.2		
298.15	1.20974	1.20916	1.21121	1.21316	1.21222	1.21186	1.21726	1.21678	1.21528
303.15	1.20684	1.20627	1.20833	1.21030	1.20936	1.20901	1.21442	1.21385	1.21243
308.15	1.20392	1.20336	1.20543	1.20742	1.20648	1.20615	1.21159	1.21103	1.20959
313.15	1.20098	1.20043	1.20250	1.20453	1.20358	1.20327	1.20874	1.20819	1.20673
318.15	1.19804	1.19748	1.19957	1.20161	1.20066	1.20037	1.20588	1.20534	1.20384
323.15	1.19509	1.19454	1.19664	1.19869	1.19774	1.19747	1.20300	1.20247	1.20095
328.15	1.19214	1.19159	1.19371	1.19577	1.19482	1.19457	1.20012	1.19960	1.19805
333.15	1.18920	1.18865	1.19077	1.19284	1.19190	1.19167	1.19724	1.19673	1.19516
338.15	1.18624	1.18569	1.18782	1.18992	1.18897	1.18878	1.19436	1.19387	1.19228
343.15	1.18328	1.18273	1.18488	1.18698	1.18603	1.18589	1.19146	1.19100	1.18940

Table 34. Raw Data Viscosity

T/K	1 : 4			1 : 4 : 0.1			1 : 4 : 0.2		
298.15	435.19	436.00	435.60	595.10	590.93	599.27	733.10	732.37	733.83
303.15	309.40	309.00	309.20	418.10	415.17	421.03	512.50	511.99	513.01
308.15	221.20	221.60	221.40	298.80	296.71	300.89	366.60	366.23	366.97
313.15	166.50	165.50	166.00	220.00	218.46	221.54	266.50	266.23	266.77
318.15	126.30	125.60	125.95	165.60	164.44	166.76	199.00	198.80	199.20
323.15	97.61	97.12	97.37	127.00	126.11	127.89	151.40	151.25	151.55
328.15	77.29	76.91	77.10	99.23	98.54	99.92	117.30	117.18	117.42
333.15	61.84	61.78	61.81	78.53	77.98	79.08	92.33	92.24	92.42
338.15	50.51	50.43	50.47	63.36	62.92	63.80	73.99	73.92	74.06
343.15	41.87	41.66	41.77	51.96	51.60	52.32	60.32	60.26	60.38

Table 35. Raw Data Refractive Index

T/K	1 : 4			1 : 4 : 0.1			1 : 4 : 0.2		
298.15	1.47976	1.47976	1.47978	1.48144	1.48146	1.48145	1.48621	1.48623	1.48617
303.15	1.47861	1.47861	1.47861	1.48029	1.48031	1.48029	1.48504	1.48503	1.48501
308.15	1.47742	1.47743	1.47743	1.47910	1.47913	1.47911	1.48385	1.48383	1.48382
313.15	1.47622	1.47622	1.47623	1.47792	1.47794	1.47792	1.48265	1.48263	1.48264
318.15	1.47503	1.47503	1.47503	1.47673	1.47675	1.47674	1.48146	1.48144	1.48145
323.15	1.47384	1.47384	1.47385	1.47554	1.47556	1.47554	1.48027	1.48025	1.48026
328.15	1.47263	1.47261	1.47263	1.47435	1.47436	1.47434	1.47905	1.47904	1.47905
333.15	1.47142	1.47140	1.47143	1.47314	1.47314	1.47311	1.47785	1.47785	1.47784